# Aircraft Distributed Electric Propulsion Technologies - A Review

Majid T. Fard, *Student Member, IEEE,* JiangBiao He, *Senior Member, IEEE,* Hao Huang, *Fellow, IEEE,* Yue Cao, *Member, IEEE*

***Abstract*—Global transportation has shifted towards electromobility to achieve net-zero emission, and in the next few decades, commercial electric aircraft is likely to become a reality. This transition has embarked on through the existing More Electric Aircraft (MEA) and the ultimate goal will be potentially achieved by hybrid-electric and all-electric airliners, along with green fuel such as green hydrogen or supercritical $CO_2$ ($sCO_2$) and its potential Gg $CO_2$[1] equivalent elimination—with or without combustion. Electric propulsion replaces conventional jet propulsors with electric fans powered by electric generators rotated by an engine, a combination of generators and energy storage, or just energy storage. An appealing idea is to distribute the electric fans along the aircraft wings or tails to improve aerodynamics, boost energy efficiency, and reduce carbon emissions and acoustic noise. Focusing on distributed electric propulsion (DEP) systems, this paper reviews the state-of-the-art advancements in aircraft electrification. Three major DEP categories, i.e., turboelectric, hybrid-electric, and all-electric propulsion technologies, are investigated. Although all of them utilize electric fans as propulsors, their system structures and power generation stages are different. Hence, comprehensive considerations are required to optimize the DEP system designs. Starting with the multifarious electrical system architectures proposed in the literature, a thorough review is conducted including the system parametric specifications, design considerations of power converters, the power electronics devices' characteristics in cryogenic conditions, and various energy storage systems. This review aims to provide a reference to researchers, engineers, and policy-makers in aviation to accelerate the progress towards future net-zero emission.**

***Index Terms*—Distributed electric propulsion, turboelectric propulsion, hybrid-electric propulsion, all-electric propulsion.**

## NOMENCLATURE

| | |
|---|---|
| **AEA** | All-electric aircraft |
| **ANPC** | Active neutral point clamped |
| **BIU** | Bidirectional interface unit |
| **BLI** | Boundary layer ingestion |
| **BPR** | Bypass ratio |
| **BWB** | Blended-Wing-Body |
| **COP** | Coefficient of performance |
| **COP26** | Conference of the Parties |
| **CSC** | Current source converter |
| **CTE** | Coefficients of thermal expansion |
| **DAB** | Dual active bridge |
| **DEP** | Distributed electric propulsion |
| **DP** | Distributed propulsion |
| **eBPR** | Effective bypass ratio |
| **EIS** | Entry into service |
| **ELDC** | Electric double-layer capacitor |
| **EMI** | Electromagnetic interference |
| **EPS** | Electric power system |
| **ESS** | Energy storage system |
| **EV** | Electric vehicle |
| **FCL** | Fault current limiter |
| **FPR** | Fan pressure ratio |
| **GaN** | Gallium Nitride |
| **GHG** | Greenhouse gas |
| **GTF** | Gas turbofan |
| **HDEP** | Hybrid distributed electric propulsion |
| **HEA** | Hybrid-electric aircraft |
| **IMD** | Integrated motor drive |
| **$LH_2$** | Liquid Hydrogen |
| **Li-ion** | Lithium-ion |
| **MEA** | More Electric Aircraft |
| **$MgB_2$** | Magnesium diboride |
| **MMC** | Modular multilevel converter |
| **Mod** | Modification |
| **MTOW** | Maximum takeoff weight |
| **MMEI** | Micro-multilayer multifunctional electrical insulator |
| **MVDC** | Medium voltage DC |
| **NASA** | National Aeronautics and Space Administration |
| **NM** | Nautical miles |
| **N3CC** | N+3 conventional configuration |
| **OEW** | Operating empty weight |
| **OMI** | One motor inoperative |
| **PAX** | Passenger count |
| **PDIV** | Partial discharge inception voltage |
| **PEBB** | Power electronic building block |
| **PMU** | Power management unit |
| **PTFE** | Polytetrafluoroethylene |
| **PWL** | Sound power level |
| **RBCC** | Reverse-Brayton cycle cryocooler |
| **$sCO_2$** | Supercritical $CO_2$ |
| **SEB** | Single-event burnout |
| **SEGR** | Single-event gate rupture |
| **SFC** | Specific fuel consumption |
| **Si** | Silicon |

M. T. Fard and J. He are with the Department of Electrical and Computer Engineering, University of Kentucky, Lexington, KY, 40506, USA (E-mail: m.fard@ieee.org, jiangbiao@ieee.org).

H. Huang is with the Department of Electrical and Computer Engineering, University of Houston, TX, 77204, USA (E-mail: hhao4@central.uh.edu).

Y. Cao is with the School of Electrical Engineering and Computer Science, Oregon State University, Corvallis, OR, 97331, USA (E-mail: yue.cao@oregonstate.edu).

[1]Gg $CO_2$ equivalents are all greenhouse gas (GHG) emissions converted into $CO_2$ equivalent so they can be compared.

This article has been accepted for publication in IEEE Transactions on Transportation Electrification. This is the author's version which has not been fully edited and content may change prior to final publication. Citation information: DOI 10.1109/TTE.2022.3197332



| | |
|---|---|
| **SiC** | Silicon Carbide |
| **SOFC** | Solid-oxide fuel cell |
| **SOV** | Safe operating voltage |
| **SPMSM** | Surface Permanent Magnet Synchronous Machine |
| **SSPC** | Solid-state power controller |
| **TEA** | Turboelectric aircraft |
| **TeDP** | Turboelectric distributed propulsion |
| **THD** | Total harmonic distortion |
| **TMS** | Thermal management system |
| **TRL** | Technology readiness level |
| **VF** | Variable frequency |
| **VSC** | Voltage source converter |
| **WBG** | Wide bandgap |

## I. Introduction

THERE has been a growing demand for increasing on-board electrical power in aircraft over the past decades due to multiple benefits. While the electric power levels for Boeing 747-100 (first flight in 1969) and Airbus A380 (first flight in 2005) were 200 kVA and 600 kVA, respectively, the electric power level of Boeing 787 (first flight in 2009) reached 1 MVA to further realize the concept of More Electric Aircraft (MEA) [1]–[3]. Aircraft electrification brings significant benefits, including much lower carbon emissions and acoustic noise, higher energy efficiency, and lower operating costs.

First, cutting the carbon footprint is of crucial importance. Currently, aviation accounts for 2.4% of global $CO_2$ emissions [4], and achieving net-zero carbon emissions by 2050 implies 21.2 gigatons of carbon abatement from now till then [5]. Flight weight reduction plays a vital role in accomplishing this goal. Assuming that an aircraft would burn an average of 0.03 kg fuel for each kilogram carried per hour, and considering the $CO_2$ emission index of 3.15 kg per kg of fuel, a 1 kg payload saved on each flight could save approximately 1700 tons of fuel and 5400 tons of $CO_2$ per year, if a worldwide annual flight time of 57 million hours is considered [6], [7].

In addition, aircraft acoustic noise is one of the imperative concerns for metropolitan health. The perceived noise levels for different aircraft classes are depicted in Fig. 1 [8]. The decreasing noise level over the years can be attributed to several factors. For example, A350 and B787 are much quieter than similarly sized aircraft due to the improved aerodynamics, advanced engines, and the use of lightweight materials [9], [10]. The use of turbofans, with higher performance and lower noise compared to turbojets, has been another key factor in reducing aircraft noise over the past several decades [11].

Furthermore, nonelectrical interconnections cause high power losses in conventional aircraft. For example, bleed air has been utilized for cabin pressurization and de-icing. Then, ram air is used for cooling down this high-pressure and high-temperature air, which is an inefficient process as it causes additional drag and increases fuel usage [12]. The conventional hydraulic and pneumatic actuators are also of low reliability, requiring frequent maintenance and prone to failure in high temperatures [13].

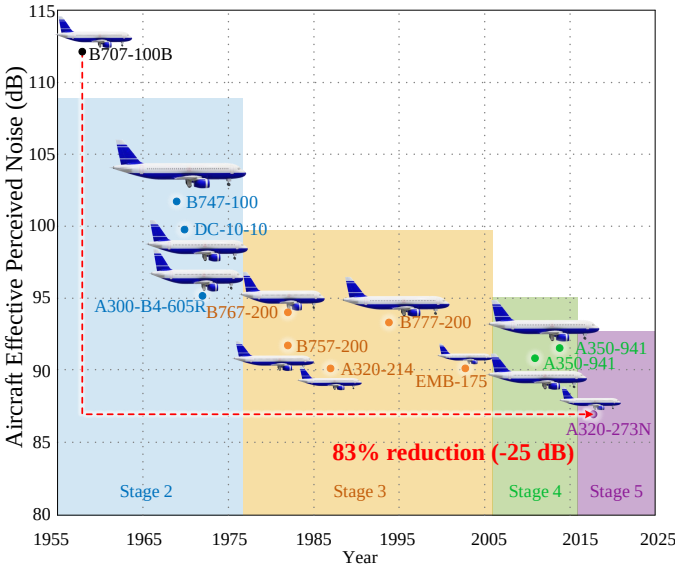


Fig. 1: Effective perceived noise of different aircraft [8].

On the other hand, in an MEA, powerful engine-driven generators feed more electrical loads. Replacing mechanical actuators with electrical ones (known as power-by-wire actuators) contributes to a mass reduction and boosts the system's reliability. To further enhance the reliability and efficiency and reduce the maintenance costs, several other non-propulsive loads, such as onboard startup batteries, de-icing system, environmental control system, flight surface controllers, fuel pumps, appliance loads, galley, control system, etc., use electric power in an MEA configuration [29], [33]. Furthermore, aircraft electrification facilitates the power and energy management and provides flexibility in power generation and remote distribution [34], [35].

Despite all the above-mentioned advancements, it is still expected that future aircraft must have much higher fuel efficiency, lower emission of air pollutants ($NO_x$ and $CO_2$), and much less noise compared to current technologies. Although it has improved aircraft performance, the focus of MEA is just on aircraft non-propulsive systems, such as hydraulic, pneumatic, and fuel systems; hence, the benefit of energy efficiency and emission reduction is rather limited. The hybrid-electric aircraft (HEA) expands electrification to a larger area of propulsion and aerodynamics for fuel burn and emission minimization, compared to that of MEA. For this reason, and to further exploit aero-propulsive interactions, distributed electric propulsion (DEP) has been proposed and has received increasing attention [36]. The DEP is a category of distributed propulsion (DP) concept in which a number of small electric propulsion units spread thrust around the aircraft wings. The goal of the DEP structure is to increase the aircraft performance in fuel efficiency, emissions, acoustic noise, landing field length, or handling performance.

Depending on the aircraft powertrain structure, the DEP can be classified into three major categories, namely, turboelectric, hybrid-electric, and all-electric configurations. The single-motor powertrain structures for each of these categories are shown in Fig. 2 with detailed explanations provided in [24].

This article has been accepted for publication in IEEE Transactions on Transportation Electrification. This is the author's version which has not been fully edited and content may change prior to final publication. Citation information: DOI 10.1109/TTE.2022.3197332



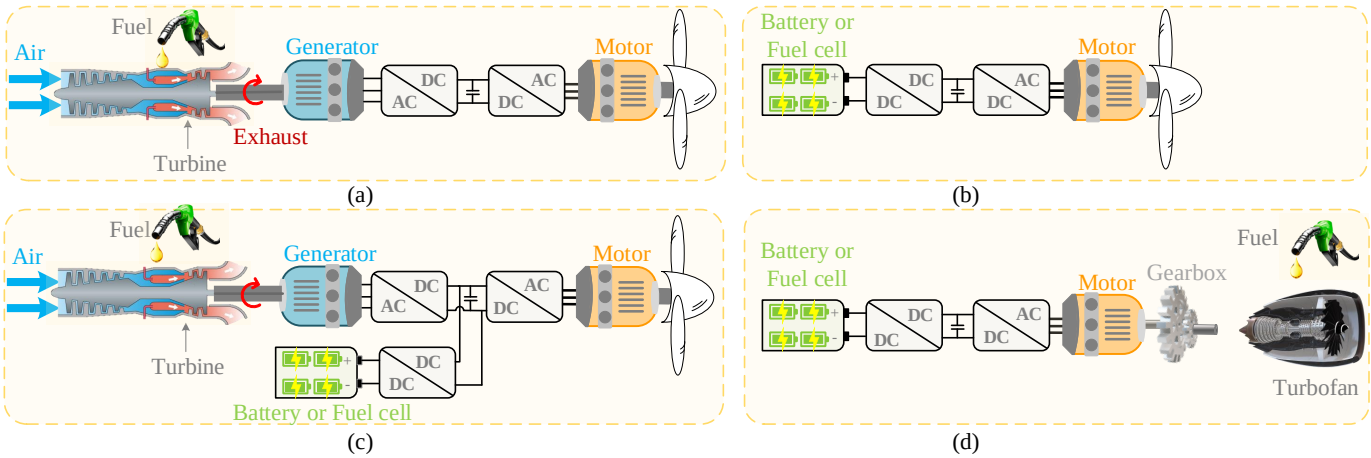


Fig. 2: Aircraft propulsion based on various powertrain structures; (a) turboelectric (b) all-electric (c) series hybrid-electric (d) parallel hybrid-electric.

The development trends and power management strategies during different mission profiles have also been elaborated, respectively, in [37] and [38], and will not be repeated here. The DEP, profoundly supported by these architectures, in conjunction with hydrogen and its potential Gg $CO_2$ equivalents elimination—with or without combustion [39]—as well as the un-ducted electric fans [40] provides the highest potential to address net-zero greenhouse gas (GHG) emission objective in 2050 set by United Nations climate change conference, COP26 [41]. Hence, extensive research on this emerging technology is necessary. Meanwhile, this requires comprehensive review papers to identify and synthesize the most recent advancements in this area.

As listed in Table I, there are a few papers in the literature reviewing electrical systems, motors, power converters, energy storage, and protection devices in aircraft. However, except [14]–[18], which focus on DEP, the rest of the papers address different aspects of MEA, AEA, TEA, or general electric aircraft without considering the effects of DEP. Among the existing DEP-related papers, the authors in [14] have discussed ongoing projects, advantages, and the challenges ahead with implementing DEP. The main focus is the aero-propulsive coupling benefits of DEP, including its integration with BLI and improved flight control. The optimization methods relevant to electric propulsion are reviewed in [15]. In [16], the historical development of distributed propulsion and challenges ahead for achieving fully-electric DP are summarized. In [17], after introducing several DP configurations, the sizing principles and digital control are reviewed.

Furthermore, there are several papers, related to electrified aircraft propulsion systems, reviewing the control methods of the motors and power converters [42], [43], system-level control methods [44], electric machines [19], [45], cables [46], circuit breakers [47], and electromagnetic interference (EMI) [48] in the literature. Therefore, these topics have been excluded from the scope of this paper.

TABLE I: Literature related to electric aircraft review with or without DEP technologies.

| Ref. | Year | Power system | Focus |
|---|---|---|---|
| [14] | 2018 | DEP | Ongoing projects, aero-propulsive coupling benefits, and improved flight control in DEP |
| [15] | 2021 | DEP | Review of optimization methods to be used in electric propulsion, and deriving optimal number of propulsors |
| [16] | 2011 | DP, DEP | Development history and challenges ahead for achieving fully-electric distributed propulsion |
| [17] | 2021 | DP | Sizing principles and digital control |
| [18] | 2013 | TeDP | Generic TeDP system, advantages and challenges of implementing TeDP |
| [19] | 2021 | General | Permanent magnet motors and magnetically geared power train for electric aircraft applications |
| [20] | 2021 | MEA | Dual inverter topologies, their design freedom, and their performance evaluation |
| [21] | 2021 | MEA, HEA, TEA | Propulsive and non-propulsive application of electric machines in an MEA and comparison between different machine technologies |
| [4] | 2021 | AEA | Reliability, efficiency, and specific power density of the EPS architectures |
| [22] | 2021 | MEA, AEA | Insulation materials and systems for electric machines, cables, and power converters |
| [23] | 2021 | MEA | Short-circuit fault current protection structures and devices |
| [24] | 2021 | MEA | Powertrain architectures, electric machines, and power converters for MEA |
| [25] | 2020 | MEA | Thermal management of electric machines |
| [26] | 2020 | General | Power electronic converters and aircraft electrification |
| [27] | 2020 | MEA, AEA | Electric power system architectures and power flow analysis of EPS |
| [28] | 2019 | MEA | Electrical machines and power electronic devices, energy management and system reliability |
| [29] | 2019 | MEA | onboard microgrids and EPS architectures, power converters, control, and protection for MEA |
| [30] | 2018 | MEA | Comparing EPS architectures for future MEA from weight and stability perspectives |
| [1] | 2018 | MEA | The evolution of the onboard DC and AC electric power generation |
| [31] | 2018 | HEA, AEA | Electrical propulsion mechanisms and energy storage |
| [32] | 2014 | MEA | Electric power system and power converters for MEA |

Different from the aforementioned papers related to DEP, this paper focuses on the review of the system architecture and specifications. Specifically, three enabling technologies for DEP are emphasized: design considerations for power electronic converters, cryogenic conditions, and energy storage. These technologies were not comprehensively reviewed in the previous literature for DEP aircraft. To this end, the rest of the paper is organized as follows. The overview of DEP and its advantages for achieving high efficiency, zero emission, and quiet flight is provided in Section II. Section III discusses the DEP architectures by presenting the possible interconnections of the distribution system. Section IV elucidates the parametric specifications of the DEP systems and the major points to be considered for system voltage selection. The design challenges of high-power converters for aircraft applications and the behavior of their components under cryogenic conditions are discussed in Sections V and VI, respectively. The benefits and barriers of embedding energy storage into the DEP are explained in Section VII. Future trends are summarized in Section VIII, and finally, conclusions and recommendations on the DEP technologies are drawn in Section IX.

## II. Advantages of Distributed Electric Propulsion

Thrust distribution for synergistic interaction with the airframe can be accomplished mechanically, using several smaller turbofan engines [49], [50], electrically [51], [52], or with a hybrid configuration [53]. Among these options, thrust distribution using electric fans is a more propitious choice to avoid the drawbacks of the mechanical system. A comparison was made between conventional and mechanical DP-based aircraft with the Blended-Wing-Body (BWB) airframe in [50], in which all candidate architectures used turbofan engines with different sizes and mounting styles. The study concluded that a mechanical DP-based configuration using internal ducts results in a heavier weight than conventional aircraft. It requires a lower propulsion system weight and specific fuel consumption (SFC) to be comparable to conventional architectures. Another issue with mechanical thrust distribution is the cumbersome gear and shaft arrangement beyond a limited number of propellers [54]. On the other hand, in DEP configuration, several electrically-driven fans can be conveniently spread out along the wings and the tail of an aircraft using power cables. This is the main reason why DEP is more favorable to aircraft designers and is gaining increasing popularity. DP and DEP provide several advantages, summarized as follows.

- *Decoupled engine and propellers*

Decoupled engine and thrust-producing mechanism in DEP allows them to operate at an optimal speed. Therefore, the engine and fans can be controlled with a variable speed ratio during the flight, which increases their efficiency and control flexibility [55], [56]. Furthermore, having several distributed motors and propellers helps to downsize the system by minimizing redundancy requirements. In order to size the electric motors of a DEP system with $N$ number of propulsors based on one motor inoperative (OMI) case, each motor should be rated at $\frac{N}{N-1}$ of the power required for the second segment climb [57]. In fact, DEP has inherent redundancy that can compensate for the thrust loss due to a propulsor failure. This can be achieved by either increasing the generated thrust of the remaining healthy propulsors or utilizing the normally-folded high-lift propellers [58].

- *Optimal allocation of propellers*

DEP provides the opportunity for optimal allocation of the propellers with varying sizes and spacing [59]. This enables several peripheral features, such as new flight control methods, boundary layer ingestion (BLI), and wake filling availability. Basic flight control can be fulfilled by coordinated modulation of the output thrust of the propeller array, obviating the need for flight control surfaces [60]. Moreover, distributing the fans along the lateral axis of the airframe enhances control flexibility and enables powered yaw control by asymmetric thrust [61]. Using differential thrust in DEP can effectively reduce the vertical tail surface area and make the rudder, ailerons, and vector nozzles trivial [62], [63].

DEP can be more conveniently integrated with the BLI technology to achieve even lower fuel consummation and higher efficiency [64], [65]. The Single-aisle Turboelectric Aircraft with an Aft Boundary-Layer propulsor or "STARC-ABL" is the most famous example of an aircraft design that uses BLI technology. As shown in Fig. 3, it has a tube-and-wing frame with two underwing turbofans that provide most of the thrust and mechanical power to the electric generators. STARC-ABL represents a simple model of turboelectric design without fully distributing the propellers. A comparison was made between STARC-ABL and the N+3 conventional configuration (N3CC) concept aircraft in [66], and significantly less block fuel burn was reported for STARC-ABL. A major part of this achievement can be attributed to the rear fuselage BLI fan, which reduces drag by ingesting the slow-moving air and helps to downsize the turbofan.

- *Higher bypass ratio*

The increased number of fans augments the total air mass flow rate through the fans and consequently enables a much higher bypass ratio (BPR). This considerably increases efficiency and quietens the flight. The effective bypass ratio (eBPR) is a parameter that considers the multiplier effect of distributing propulsors in BPR. It is defined as the ratio of the air mass flow rate through all fans to the air mass flow rate through the turbogenerators [68]. While the BPR of the B787 turbofan engine is around 10 [69], an eBPR of 36 was reported for NASA's N3-X concept, which employs a turboelectric distributed propulsion system [70]. A higher eBPR can enhance propulsive efficiency by 4-8% [71]. This number can be greatly increased while an


Fig. 3: STARC-ABL aircraft designed by NASA with a rear-mounted boundary layer ingesting fan [67].

un-ducted, distributed, and electrically driven fan concept is implemented.

- *No power lapse at altitude for all-electric configuration*
While, due to the reduced air density, conventional air-breathing engines experience power lapse at altitude, there is no such issue with electric propulsion motors. Therefore, with proper thermal management, the available power of the DEP would be independent of altitude variations or hot day conditions [72]–[74].
- *Noise reduction*
The airflow through the aircraft structure causes fluctuating pressure disturbances and generates noise. The noise emanated from an aircraft is mainly due to two main sources: the engine and the airframe. Further noise abatement is possible with the designs integrating the propulsion system and airframe together [75], [76]. Noise estimation analysis for turboelectric distributed propulsion (TeDP) and all-electric aircraft (AEA) with conventional tube and wing airframe of A320 was conducted in [77]. In comparison with the baseline A320, both DEP configurations showed lower sound power level (PWL) at takeoff, which was attributed to the higher airflow traversing the DEPs. The TeDP was estimated to generate slightly lower noise compared to the baseline A320 due to its lighter weight and reduced propulsor noise. However, the all-electric design with the existing battery technology was found to be noisier at approach because of its higher weight. In [78], a significant noise reduction of 30 dB was reported compared to that of the baseline BWB aircraft with no flaps or slats. This remarkable noise abatement was achieved by distributing multiple ultra-high-BPR engines embedded into the BWB airframe to enable the BLI and taking advantage of the shielding effects of the airframe.
Besides the reduced blade tip speed or jet exit velocity, the airframe wetted area reduction can also be attained by distributed propulsion, which consequently lowers the airframe noise [79].
- *Shorter takeoff and landing*
Another advantage of the DEP can be seen in the shorter takeoff and landing of small passenger aircraft. Using the Tecnam p2006t airframe with two propellers as a baseline, a comparative study has been conducted in [80] to evaluate aircraft performance while retrofitting distributed electric propulsion. The optimization results show that a fully blown wing with distributed propellers can potentially reduce the takeoff distance by up to 50%. As a modified version of Tecnam p2006t, X-57 *Maxwell* aircraft uses small electrically-driven high-lift propellers to achieve augmented lift during the low-speed operation [81]. Installing distributed fans on the upper surface and near the trailing edge, as in N3-X or other BWB airframes, may enhance the lift-to-drag (L/D) ratio by 8-16% through the upper surface blowing technology [71]. Taking advantage of the Coanda effect, this technology converts a portion of the thrust to lift by downward deflecting the exhaust flow at the trailing edge. Hence, improved low-speed performance by enabling shorter takeoff and landing can be achieved [82].

It should also be mentioned that the operating empty weight (OEW) of a DEP aircraft is generally higher due to the additional weight of the electrical system and propellers. However, the target is to make the maximum takeoff weight (MTOW) comparable by saving the block fuel in DEP and compensating for the additional weight of the electrical system [65]. Simply distributing propellers along the wingspan, without considering the synergistic design and aero-propulsive interactions, such as that in [84], may even lead to an infeasible or less effective design.

## III. Propulsion Architectures

The onboard power grid of the aircraft shows a high resemblance to those islanded microgrids in the terrestrial or marine industry by having generators, a power distribution system, protection devices, and various types of loads [29], [85]. However, higher reliability, specific power, and power density are unique and indispensable requirements for the aircraft, and the need for both AC and DC power with variable load priority makes this system more complicated. Several system architectures with different numbers of generators, propellers, power converter types, and other factors have been studied in the literature. The available system architectures for three types of DEP systems—turboelectric, hybrid, and all-electric—will be introduced and discussed in this section.

### A. Turboelectric DEP

In [83] and based on NASA's N3-X hybrid wing body aircraft concept, power system evaluation studies were conducted on a cryogenic TeDP system and five different power system architectures were proposed; their baseline DC power distribution system (half-circuit) is shown in Fig. 4. Here, each engine is designed to provide 25 MW (33,526 hp), the total power required at the second segment climb. The system voltage level of 1-10 kV and all-cryogenic system components were considered in the cryogenic TeDP. Using redundant units, a fail-safe design approach was adopted for all electrical power components. Specifically, two generators/converters with two separate transmission lines for each engine are utilized to increase the fault resiliency. In the distribution section, four DC buses (2 per half-circuit), to which the energy storage units are also connected, are feeding the independent wing

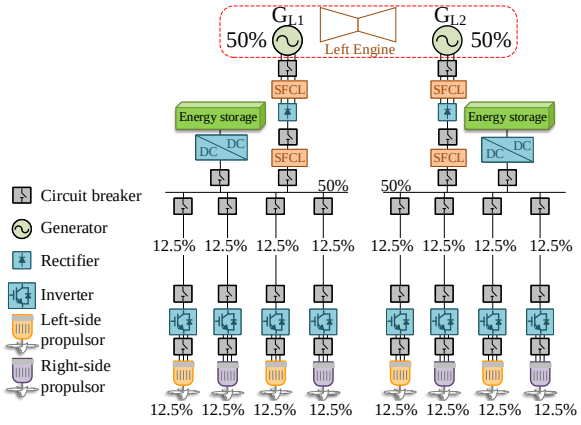


Fig. 4: Baseline propulsion system architecture (half-circuit) [83].

transmission lines without any interconnect or bus tie. There are 16 propulsors (8 per half-circuit), including DC-AC drives, AC motors, and fans (symmetrically assigned to the distribution buses), and each propulsor is rated at 1/8 of the minimum power requirement. The propulsors' arrangement over the wings is such that in case of an engine failure, the remaining unaffected propulsors can still provide nearly symmetrical thrust.

The main idea which distinguishes the proposed architectures is using a bus tie or routing the power between the buses to achieve an optimum size and weight for the system (See Fig. 5). The specific level of interconnectivity in radial architectures has the major advantage of reducing propulsor and distribution line power ratings [86]. Extra interconnectivity, on the other hand, may increase system weight and complexity without considerable advantages. As an instance, a "*dual Inner Bus Tie*" architecture with two bus ties was proposed in [87]. Although the healthy engine can power all the motors in case of an engine failure, further motor rating reduction is not possible with that architecture.

In [36], three different topologies, i.e., DC, AC-DC, and AC architectures, were compared from the weight and efficiency perspectives. The AC-DC and AC architectures are shown in Figs. 6 and 7, respectively. The role of the energy storage units in Fig. 6 has not been defined clearly, but in TeDP systems, they are generally used for non-propulsive purposes only. In [36], the AC circuit-breakers were also not included in the AC-DC and AC architectures, but they are necessary to protect EPS and isolate defective parts from the rest of the system. In the AC-DC configuration, the power is distributed in AC form and a back-to-back propulsion drive is developed for each motor, while in the AC one, there is no power conversion stage, and the motors are directly coupled with the generators through the AC bus. As it will be shown in Fig. 15 and compared in Table II, the AC system has a significantly lower weight than the other ones, mostly because it does not need power electronic converters. In fact, power electronic converters have a substantial impact on system mass and full-load losses.

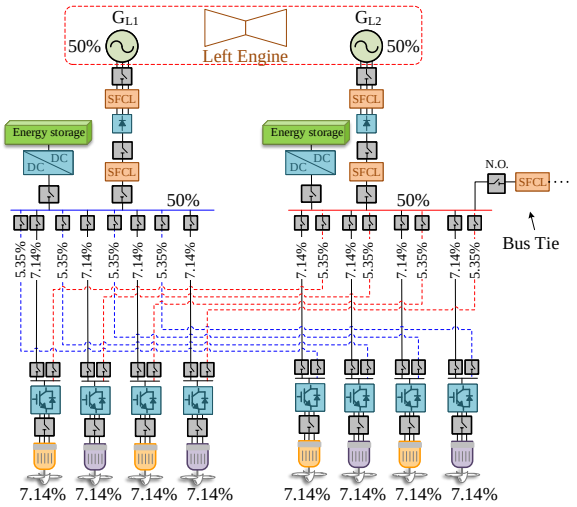


Fig. 5: Four-bus inner bus tie multifeeder architecture (half-circuit) [83].

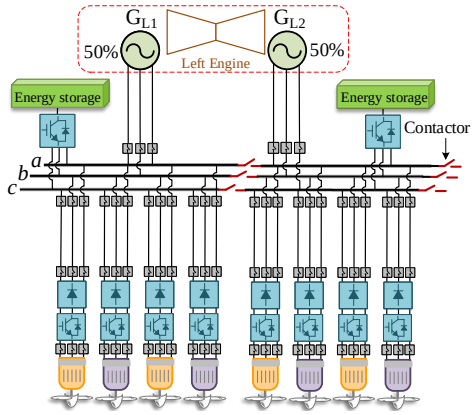


Fig. 6: AC-DC architecture (half-circuit) with AC main bus, and a back-to-back converter for each motor [36].

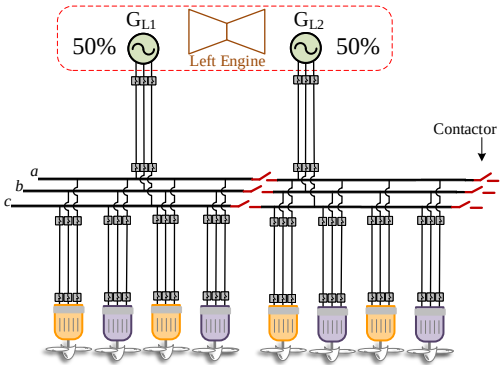


Fig. 7: AC architecture (half-circuit), which does not have any converter [36].

Nevertheless, power converters are of utmost significance, since they provide decoupling between the generators and the motors, and they also provide a high degree of controllability to the system.

Besides voltage source (VS) architectures, a current source (CS) configuration was also presented in [54]. The *3-Bus Multifeeder* voltage source and the current source architectures are depicted in Figs. 8 and 9, respectively. The substantial improvement achieved in these types of *Multifeeder* configurations is that they replace most of the bulky circuit breakers of the previous architectures with lightweight superfast disconnectors. On the other hand, using bidirectional bus interface units (BIU) as shown in Fig. 9, ring buses were created in the CS-based system, where bypass switches would be used for fault isolation purposes. Both architectures are lighter than the baseline one, but the VS-based system is recommended due to its slightly lower weight, power rerouting capability, and less insulation required at higher voltage levels compared with the CS architecture.

Moreover, three types of microgrids, i.e., AC, DC, and AC-DC, were proposed for the ECO-150 aircraft and compared in terms of mass and efficiency in [88]. ECO-150 is a 150-PAX concept aircraft being developed by Empirical Systems Aerospace, Inc. (ESAero) since 2008. Several variants of this TeDP concept have been considered with cryogenically and non-cryogenically cooled systems. The TeDP-based ECO-150-

This article has been accepted for publication in IEEE Transactions on Transportation Electrification. This is the author's version which has not been fully edited and content may change prior to final publication. Citation information: DOI 10.1109/TTE.2022.3197332



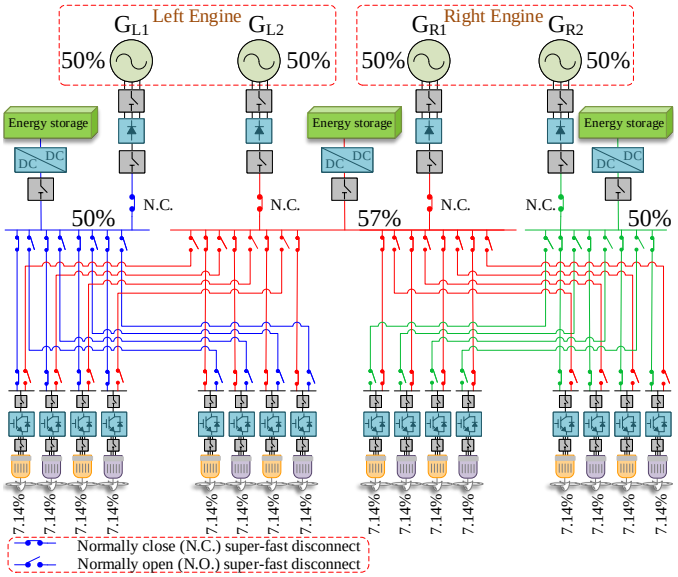


Fig. 8: Voltage source-based three-bus multifeeder architecture using lightweight super-fast disconnectors [54].

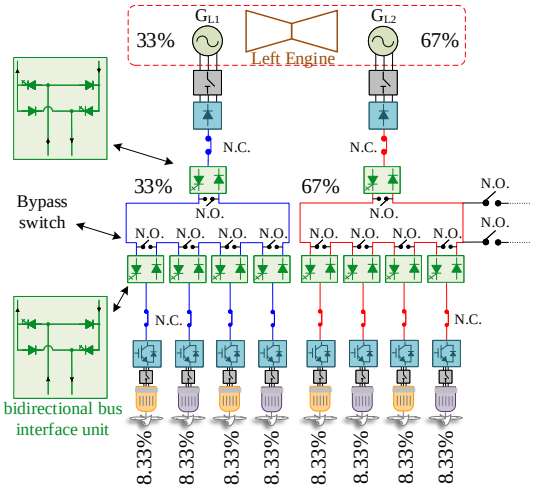


Fig. 9: Current source-based propulsion architecture (half-circuit) [54].

300, which is shown in Fig. 10, uses a split-wing airframe and non-cryogenic cooling technology with conventional electric machines [87]–[89]. The schematic of the AC-DC architecture is depicted in Fig. 11, where the inboard propulsors are directly connected to the AC buses, and the outboard ones are fed from the rectifiers and motor drives. The other two architectures investigated in [88] (AC and DC architectures) are also similar to the diagram shown in Fig.11 in having four separate buses with a bus tie between the middle buses. In comparison, AC architecture yields the lightest weight and highest efficiency, but it suffers from limited yaw-control flexibility. The DC architecture was proved to be 2-3% less efficient compared with the AC one. However, it has better yaw control capability and becomes the most lightweight architecture at voltages above 3 kV. Compared with the other designs, the AC-DC architecture showed an unsatisfactory performance from both the mass and efficiency perspectives.

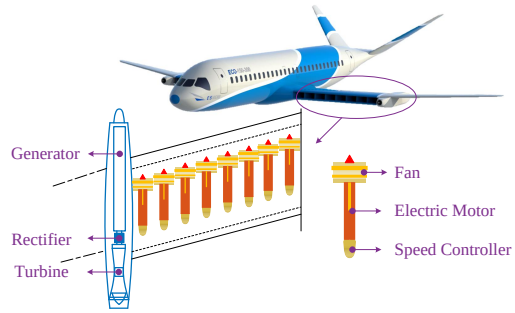


Fig. 10: ECO-150-300 aircraft with its split-wing design and 16 ducted fans developed by ESAero [90], [91].

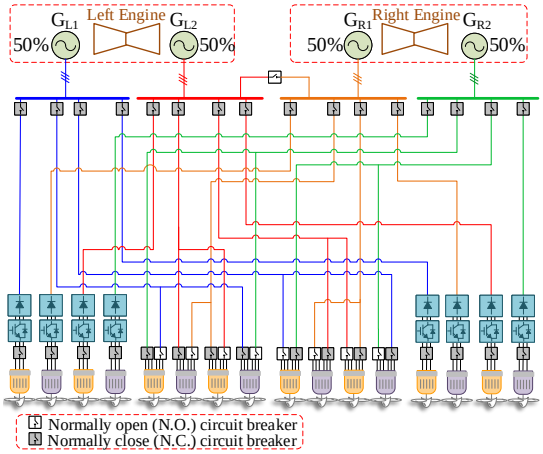


Fig. 11: TeDP topology with an AC-DC architecture. Inboard propulsors are directly connected to the AC buses and outboard ones are being fed from the rectifiers and motor drives [88].

Based on the experience gained from the all-electric AMPERE project (See Subsection III-C), ONERA launched another concept aircraft called DRAGON (Distributed fans Research Aircraft with electric Generators by ONERA) which is shown in Fig. 12. DRAGON is a 150-PAX turboelectric aircraft concept with a range of over 800 NM that uses generators coupled to the turboshaft engines [92], [93].

As depicted in Fig. 13, a baseline power system architecture was studied for DRAGON in [93] where four electric generators are connected to AC buses through circuit breakers. Batteries or energy storage units are not utilized in the propulsion chain, due to their low specific power and considerable weight penalty in large passenger aircraft. Therefore, despite

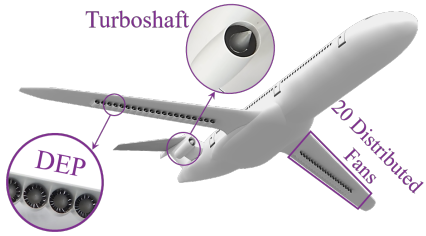


Fig. 12: DRAGON concept aircraft, being developed by ONERA, with tube and wing airframe and 40 small fans distributed on the pressure side of the wings in the rearward position [92].

This article has been accepted for publication in IEEE Transactions on Transportation Electrification. This is the author's version which has not been fully edited and content may change prior to final publication. Citation information: DOI 10.1109/TTE.2022.3197332



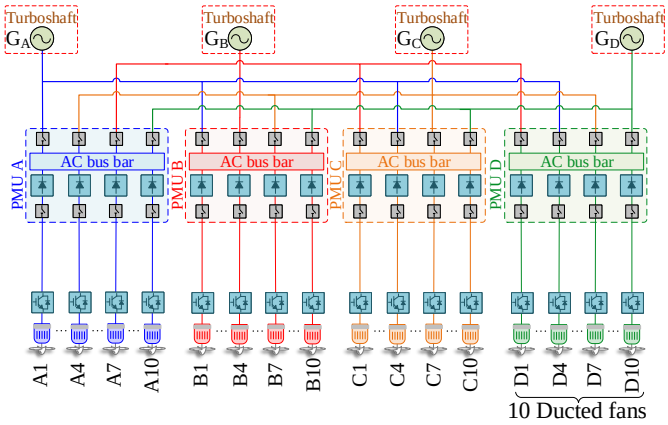


Fig. 13: Power architecture for DRAGON concept aircraft [93].

being called a hybrid-electric aircraft by its developers, it falls into the TeDP category based on Fig. 2. Each AC bus with its associated four AC-DC converters forms a power management unit (PMU). The PMUs reconfigure the distribution system after an engine failure so that the affected bus can still be powered using the other three healthy engines. Three possible technology evolution scenarios, i.e., "Negligible", "Moderate", and "Significant" with entry into service (EIS) by 2035, were considered in [93] and weight estimation studies were carried out. Each scenario defines different specifications for the specific power and efficiency of the components. It was found that the "Moderate" evolution of the electric components would bring about an 8.5% fuel burn reduction for DRAGON compared with the conventional tube and wing configuration at that time. This holds as long as the design range is below 1100 NM. Otherwise, the "Significant" evolution in the specific power of electric components is required for the DRAGON to prove more efficient than conventional aircraft. Furthermore, while the DEP is expected to be more efficient than the classical turbofan during cruising, the results however, indicate that DEP has lower efficiency than the classical turbofan during cruising mode, and improved performance is achieved only during climbing.

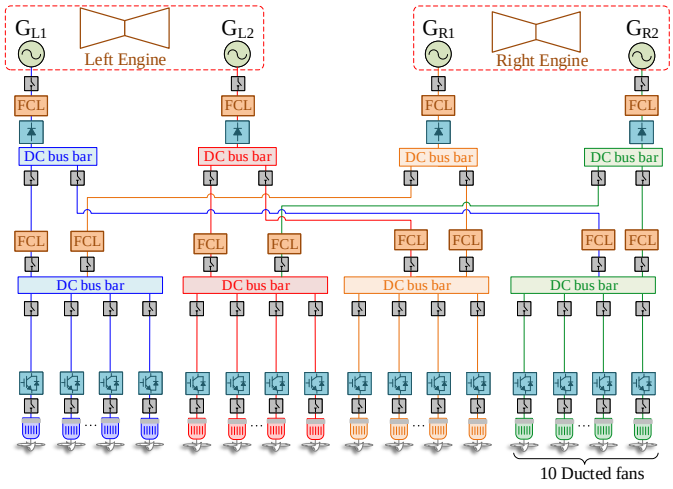


Fig. 14: Cross-redundant architecture for DRAGON aircraft [94].

To avoid oversizing the power components, the architecture shown in Fig. 13 was replaced by a cross-redundant architecture proposed in [94] and depicted in Fig. 14. AC buses are replaced by DC ones, and fault current limiters (FCL) are added to this architecture. It was designed in such a way that in case of an engine failure the remaining can power all ducted fans.

Fig. 15 and Table II are provided to summarize and compare the architectures presented. Specifically, the weight and component count of different cryogenic-based TeDP architectures are provided in Fig. 15. The maximum required power is assumed to be 25 MW for all architectures. Although energy storage and fault current limiters are excluded from weight comparisons, they have been considered in component count analysis. The generators have an equal impact on all architectures. Architectures **A**, **B**, and **E** have higher extra propulsive power and therefore higher motor weight. Power converters have the greatest impact on the DC systems' weight. This is due to their low specific power and a high number of required rectifiers and inverters in these architectures. Among DC architectures, **D** and **E** have the lowest weight owing to replacing most of the DC breakers with lightweight disconnectors and a lower number of BIUs, respectively. The total weight of the bus, transmission, and feeder cables is almost the same for all architectures. Multifeeder architectures have a high number of cable connections; however, the lower power rating of the cables in these architectures reduces their additional weight. AC and AC-DC architectures, on the other hand, have considerably lower weight and component count among others. This is mainly due to the elimination or reduction of the power converters and the higher specific power of AC breakers compared to the DC ones. It should be mentioned that the assumed specific power levels are estimated values

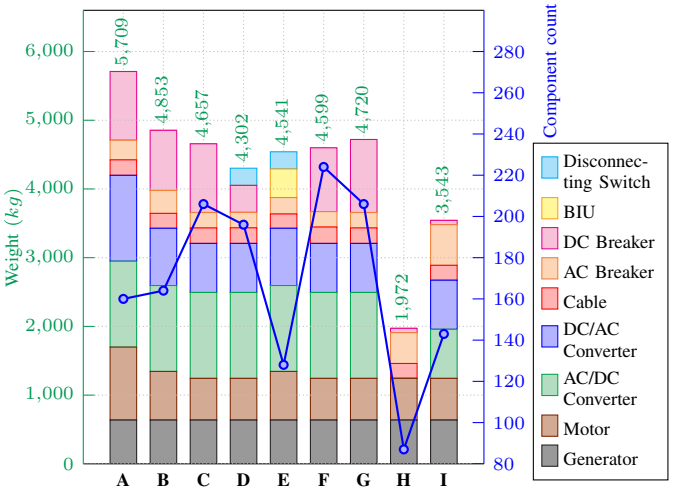


| | | | |
|---|---|---|---|
| **A** | Baseline (Fig. 4) | **F** | Cross-redundant [83] |
| **B** | Inner bus tie [83] | **G** | 4-bus/bus tie multifeeder (Fig. 5) |
| **C** | 3-bus/multifeeder [83] | | |
| **D** | 3-bus/disconnectors (Fig. 8) | **H** | AC (Fig. 7) |
| **E** | Current Source/BIUs (Fig. 9) | **I** | AC-DC (Fig. 6) |

Fig. 15: Weight and component count comparison of different cryogenic EPS architectures for DEP.

based on [54]. Further evaluation of these architectures from various perspectives is provided in Table II, at the end of this section.

### B. Hybrid-electric DEP

Using the concept of HEA, it is possible to reduce the carbon footprint and maintain a longer range of flight compared to an all-electric aircraft. For instance, the EcoPulse™ is a distributed hybrid-propulsion aircraft demonstrator, with its first flight scheduled in 2022. A turbogenerator drives the main rotor on the fuselage and charges the batteries supplying power to six electric motors, each of which is rated at 50 kW. The motors are connected to the propeller fans mounted on the leading edge of the wings. Here, the DEP is expected to improve the aircraft's performance, lower the noise, and save energy in this hybrid-electric aircraft [95], [96]. Recently, Airbus has developed light-weight, high-voltage Li-ion batteries to be tested on EcoPulse aircraft. The battery pack weighs 350 kg with 800 VDC maximum voltage and 350 kW output power [97].

In [98], it was found that the designed HEA with 40 propulsors, 2 generators, 4 battery packs, and 28 MW of minimum takeoff power is feasible for ranges below 1,200 NM. The takeoff and climb phases are designed to be fully electric with batteries, but the batteries are not employed during the cruising mode due to the increased weight of the aircraft. Instead of using a degree of hybridization, where each energy source provides a certain amount of power in any specific flight stage, the power management strategy is defined separately for different energy sources. This is advantageous, as it increases the robustness of the system against failures. Using this strategy, cases with one inoperative generator or two inoperative battery packs were investigated using a simple fuel breakdown analysis.

The authors in [99] proposed a hybrid-electric DEP concept, in which the propulsive system architecture is depicted in Figs. 16 with two turbogenerators connected to all buses and batteries integrated into the system on the AC side of the PMUs. Optimization studies, considering the fuel and energy

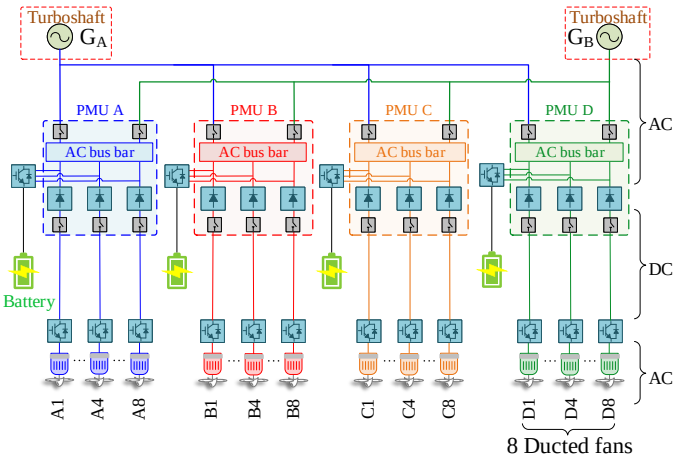


Fig. 16: Power architecture of an HEA with battery stacks connected to the AC bus of the PMUs [99].

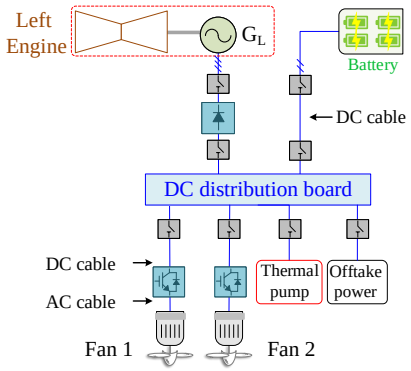


Fig. 17: Hybrid-electric aircraft power system architecture (half-circuit) proposed in [101].

consumption for configurations with 16, 32, and 48 electric motors, were carried out. It was found that the case with 32 motors offers the most satisfactory results, and the hybrid aircraft is more advantageous in short-range flights due to the weight penalty of the batteries.

Within the turboelectric aircraft design environment (TRADE) Clean Sky 2 program in Europe, several universities collaborated to develop a design and optimization platform for specific 190-PAX aircraft technologies [100], [101]. Half of the onboard electric power system architecture used in this study is illustrated in Fig 17, in which a boosted gas turbofan (GTF) feeding an oil-cooled SPMSM and a battery pack are the available power sources. In each half-circuit, the loads include two ducted electric fans connected to SPMSMs, a thermal pump for the thermal system, and an offtake for secondary loads. The research study shows that the energy density of the battery pack, the power rating of the electric fans, and the power split ratio between the battery pack and the generator have a great influence on the overall mass and fuel consumption.

According to the literature ( [98], [99], [102]–[104]), achieving a high percentage of hybridization in cruising mode while maintaining the same range as that of conventional aircraft would be very challenging without substantial technological developments, especially in the battery's specific energy.

### C. All-electric DEP

Since 2013, a DEP project called AMPERE has been studied by ONERA®, a French aeronautics research laboratory [93], [105], [106]. Although it has been widely referred to as a hybrid-electric topology in literature, the AMPERE is essentially an all-electric aircraft based on the classification provided in Fig. 2. AMPERE, a 4-6 PAX concept aircraft with 400 kW of peak power, is powered by fuel cells and Lithium-ion (Li-ion) batteries that drive 40 electric ducted fans [105]. The modular power distribution architecture proposed for this aircraft is depicted in Fig. 18, in which 10 hydrogen tanks supply the fuel cells, and each fuel cell unit is bundled with a battery to form a cluster. Each cluster feeds four DC-AC inverters distributed symmetrically across the wings. Two different voltage levels are used in this architecture: high voltage 135 VDC and low voltage 28 VDC for primary and

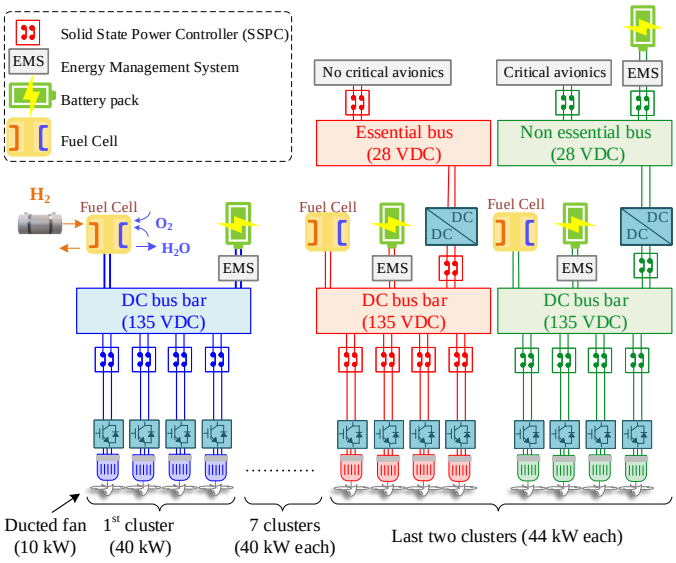


Fig. 18: Modular architecture proposed in [105], [107] for ONERA's AMPERE aircraft concept.

secondary distribution systems, respectively, and solid-state power controller units are used for load control and protection purposes [107].

The X-57 *Maxwell* is another all-electric experimental aircraft developed by NASA to achieve higher aero-propulsive efficiency compared with the gas-powered Tecnam P2006T as a baseline [52], [108]. This configuration is being developed under four modification (Mod) stages. Mod IV has two electric motors for the cruising mode, each of which is rated at 72 kW on the wingtips, as well as 12 smaller motors (10.5 kW each) installed on the underwing pods employed only during takeoff and descent. The use of distributed fans along with the cruise wing tip propellers helps reduce the induced drag and improves the high-lift capability [109]. Two independent Li-ion battery packs with a total usable energy of 47 kWh are the only onboard power supplies [110]. The traction system architecture is shown in Fig. 19.

The nominal voltage of the batteries and main DC-buses is 461 VDC, and motor torque controllers connected to these buses are driving the cruise motors. Two DC-DC buck converters are utilized to generate the 14 VDC for the avionics, and a DC-DC boost converter stage is used to provide 28 VDC for the instrumentation. An important point to note with this design is the fair amount of redundancy considered for all safety-critical components to minimize the impacts of single-failure modes. As can be seen in Table II and compared with the architecture shown in Fig. 18, this one has more interconnectivity and extra propulsive power, but it will have a lower range and payload due to using batteries as the only energy source. Comparing AMPERE's and X-57's system structures, both are relatively complicated. Namely, the AMPERE aircraft (Fig. 18) due to its two types of energy sources and energy management systems and the X-57 aircraft because of using different motors and their management in different phases of the mission profile.

## IV. DEP System Parametric Consideration

Voltage levels for the electric power system (EPS) affect the overall electrical design of the aircraft: from the size and number of the generators and motors to the type of the distribution system and power converters. Parametric specifications of the DEP system architectures mainly include the voltage and current levels, and the operating frequency. For a given power capacity, once the voltage level is determined, the current ratings will be specified accordingly. While it is necessary, there are not available voltage standards for DEP systems. Such standards can be adopted from the existing standards by considering the similarities between the DEP-based aircraft power distribution network and those of conventional aerospace, terrestrial, and marine industries [85]. Conventional commercial aircraft, such as A320, A330, and A340, typically use an AC line-to-neutral voltage of 115/200 V with a line frequency of 400 Hz. Variable frequency (VF) systems were also deployed in the A380, A350, and Boeing 787, with a frequency ranging from 360 to 800 Hz [3]. In addition, there is a trend in increasing aircraft systems' voltage level over the past decades [1], from 270 VDC to 540 VDC, or even higher voltages. This is in response to the increasing electric power demand in MEAs and an appeal for designing highly efficient systems. Here in this section, a high-level view of medium-voltage DC (MVDC) and cryogenic aircraft systems will be provided.

### A. MVDC as a possible future solution

A DC system may be preferred due to its control flexibility, decoupling feature, lower cable weight, and cost, despite its higher mass and losses compared to an AC distribution system. Currently, the highest DC voltage utilized in a commercial aircraft can be found in Boeing 787, with 540 VDC ($\pm$ 270 VDC) supplied from four auto-transformer rectifier units that convert 235 VAC to $\pm$ 270 VDC [1], [111].

However, severe operating conditions at higher altitudes with lower air pressure add a constraint to the system voltage. According to Paschen's Law, which relates the partial discharge inception voltage (PDIV) to the distance between the electrodes ($d$) and the air pressure ($P$) at room temperature, the low pressure at the operating altitude of the commercial aircraft decreases the PDIV. However, Paschen's Law is for the case that uses uninsulated conductors [112]. The insulation material would decrease the total fraction of the wire voltage across the air gap ($f_V$) as:

$$f_V = \frac{d}{d + (t_i/\varepsilon_r)} \tag{1}$$

where $t_i$ and $\epsilon_r$ are the insulation thickness and relative permittivity, respectively. Equation (1) is based on a uniform electric field assumption and for cable-to-ground calculations. Insulation thickness should be doubled for cable-to-cable analysis. Then, instead of the breakdown voltage ($V_{bd}$) calculated for the air insulator, a safe operating voltage ($SOV$), as defined below, would be used as the high-voltage limit of the system [113].

$$SOV = \frac{V_{bd}}{f_V} \tag{2}$$

This article has been accepted for publication in IEEE Transactions on Transportation Electrification. This is the author's version which has not been fully edited and content may change prior to final publication. Citation information: DOI 10.1109/TTE.2022.3197332



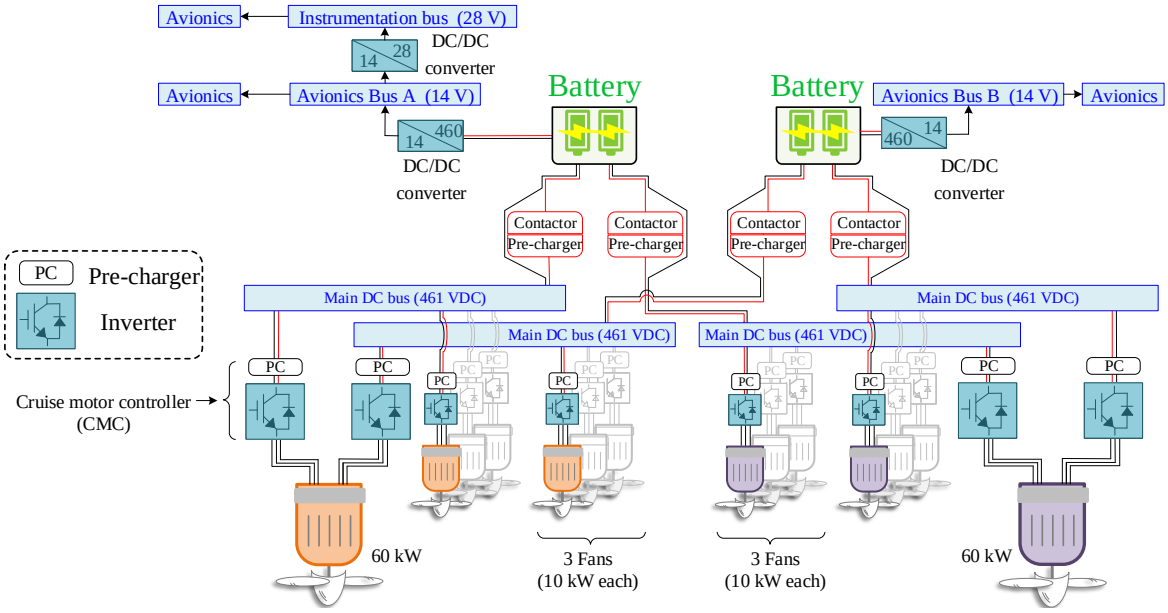


Fig. 19: Traction system architecture of NASA's X-57 (Mod IV) all-electric aircraft [52].

TABLE II: Electric power system architecture comparison for different DEPs.

| Powertrain | Reference | Weight | Reliability (Interconnectivity) | System Complexity | Extra Propulsive Power | Component Count | Failure Reconfiguration complexity | Multiple sources on common bus | Control Flexibility |
|---|---|---|---|---|---|---|---|---|---|
| Cryogenic TEA | Baseline (Fig. 4) | High | Low | Medium | High | Medium | Low | Low | High |
| | Inner bus tie [83] | High | Medium | Medium | Medium | Medium | Medium | Medium | High |
| | 3-bus multifeeder [83] | High | High | High | Low | High | High | High | High |
| | 3-bus with disconnectors (Fig. 8) | Medium | High | High | Low | High | High | High | High |
| | Current Source with BIUs (Fig. 9) | High | High | High | Medium | Medium | High | Medium | High |
| | Cross-redundant [83] | High | High | High | Low | High | High | High | High |
| | 4-bus with bus tie multifeeder (Fig. 5) | High | High | High | Low | High | High | High | High |
| | AC (Fig. 7) | Low | Medium | Medium | High | Low | Medium | Medium | Low |
| | AC-DC (Fig. 6) | Low | Medium | Low | High | Medium | Medium | Medium | High |
| Non-Cryogenic TEA | Fig. 11 | Low | Medium | Medium | Low | Low | High | Medium | Low |
| | Fig. 13 | Medium | Medium | Medium | Medium | Medium | Medium | High | High |
| | Fig. 14 | High | Medium | High | Medium | High | Medium | Medium | High |
| HEA | Fig. 16 | High | High | High | Low | High | High | High | High |
| | Fig. 17 | Low | Low | Low | High | Low | Low | Low | Low |
| AEA | Fig. 18 | Low | Low | High | Low | High | Low | Medium | High |
| | Fig. 19 | High | High | High | High | Low | High | Medium | High |

Assuming a constant pressure of 11.6 kPa, the airgap breakdown voltage (Paschen's law) and the SOV using a PTFE insulator are compared at different airgap lengths as shown in Fig. 20. The insulation thickness is 0.31 $mm$, and $\varepsilon_r$=2.1. It can be seen that the minimum PDIV has increased more than two times, and it occurs at a longer airgap distance.

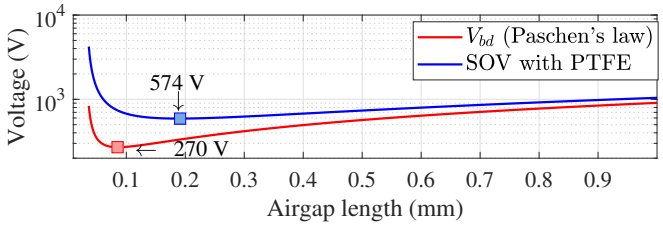


Fig. 20: PDIV with air insulator and PTFE insulator at different airgap lengths.

Obviously, unlike high-voltage in terrestrial, shipboards, or train applications, there is a limit on creepage or clearance distances and using overdesigned heavy systems in aircraft applications. Therefore, ameliorated insulators with improved materials are also required to increase the SOV. These insulators must be tested in multiscaled, multi-stressed, and accelerated conditions to replicate a real flight and degradation phenomena. An example of a promising insulator is the micro-multilayer multifunctional electrical insulator (MMEI) system, which is a state-of-the-art technology expected to improve the insulation performance from several aspects like corona discharge, EMI issues, moisture blocking, heat dissipation, etc. [114].

Although system voltage affects the mass of other components like motors and power converters, the cable mass is generally the most sensitive parameter to the system voltage, and it changes considerably in non-cryogenic systems. There-

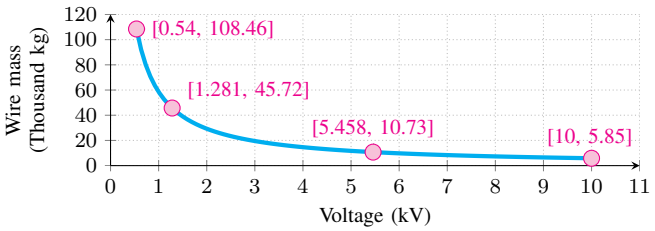


Fig. 21: System voltage vs. cable weight (no dielectric insulation considered) [115].

fore, the change of the estimated wire mass with increasing system voltage is shown in Fig. 21 for a 100 MW notional aircraft [115]. Estimation is based on $8\times45$ $m$ copper conductors (with approximately 614.62 A/kg/m) without insulation weight. Here, the conductor core weight reciprocally drops with system voltage (Weight $\propto$ Voltage$^{-1}$), giving rise to the increase in the specific power. Although higher voltage results in lightweight conductors, it requires thicker insulation with larger creepage and clearance distances, which in turn will compromise the gravitational and volumetric power densities of the system [116]. However, the total cable mass and consequently, the total system mass will be reduced.

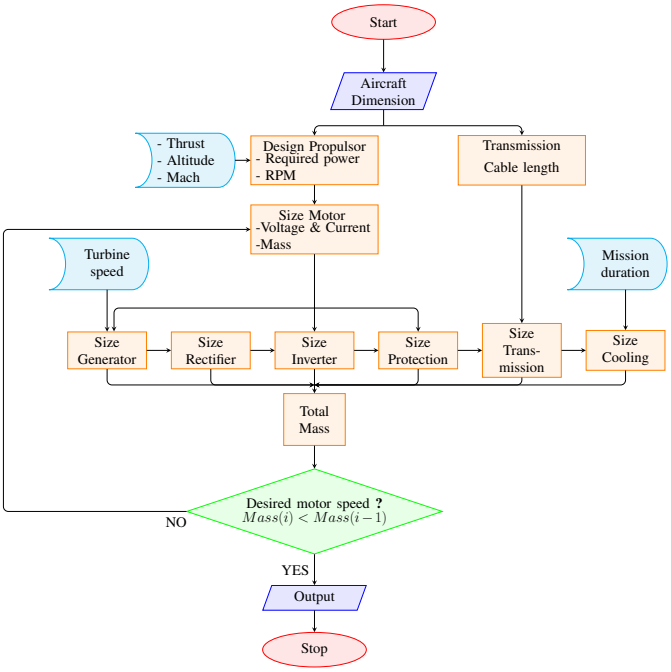


Fig. 22: Flowchart of the aircraft components sizing process to derive optimal voltage and current proposed in [117].

### *B. Voltage level of existing DEP technologies*

In Table III, specifications for some DEP-based aircraft topologies, including their power levels and system voltages, are presented. While TeDP is used for high-power and large aircraft, medium- and small-sized systems are designed based on HEA and AEA architectures, respectively. This is due to first, the low specific energy density of batteries and their "hidden" weight that needs to be carried even after being discharged. Hence, with current technology, batteries are infeasible in high-power, long-range aircraft designs. Second, battery packs have limited output voltage. As can be inferred from Table III, the voltage level in megawatt-scale aircraft systems is usually increased to over 1 kV to optimize the electrical systems (e.g., weight and specific power) and reduce overall power losses. However, the 800 VDC battery pack to be tested on EcoPulse [97] is the highest voltage supplied by batteries in the aerospace industry. Higher voltage batteries could increase safety risks and require complicated thermal management systems to prevent thermal runaway.

In [117], an optimal voltage level selection procedure for a non-superconducting turboelectric system was proposed. As shown in Fig. 22, first, the propulsor size is estimated based on the aircraft size and the required thrust. Then, the required rotational speed of the propulsor to provide the thrust and the motor size are calculated. Finally, the voltage of the motor driving the propeller is imposed on the electrical system to size the other components. The process will be repeated until the optimal mass is obtained. The results show that the mass of the electric machines and the cooling system would be considerable at low speeds and voltages. However, at high speeds and voltages, the power electronic devices may have a greater contribution to the overall system weight. First, this algorithm is taking sequential sizing steps, which cannot take the design interdependency between different components into account. Second, the algorithm considers a fixed number of propulsors in the "design propulsor" stage, which can provide the required thrust at different rotational speeds. Applying this optimal-voltage derivation algorithm to DEP with the flexible number of propulsors will require an additional stage of optimization to find the optimum number of propulsors. Therefore, for DEP, an optimization process is required to optimize the number of propulsors and other system specifications simultaneously. Due to the high complexity and calculation burden, heuristic and multidisciplinary optimization algorithms could be more efficient and authentic [118].

According to Table III, cryogenic design has been used only for high-power systems, such as those with tens of megawatts. Typically, a non-cryogenic system is preferred in aircraft designs. However, if high onboard power is required, the high efficiency of a cryogenic system outweighs its complexity, stability issues, required change of design and infrastructure, and reliability challenges. The decision to use a cryogenic or non-cryogenic system can dictate the voltage level selections. In a non-cryogenic system, increasing the voltage level leads to a lower current at the same power rating, and thus lowers the size and ohmic losses of the conductors [128]. Using a cryogenic system and pressurized environment, however, will allow the ohmic losses of the superconducting cables, motors, and all other components inside the cryogenic chamber to be negligible. Therefore, the current level could be increased until it gets closer to the critical current of the superconductor [54].

The challenge with using cryocoolers or pressurized chambers is the increased mass and failure probability of the system due to the added components. The mass of a Reverse-Brayton cycle cryocooler (RBCC) system can be estimated as [129]:

TABLE III: Specifications of some distributed propulsion aircraft in the literature.

| Reference | Model | Powertrain architecture | Power level† | PAX | System voltage | Cryogenic (C) or Non-cryogenic (NC) | Number of propulsors |
|---|---|---|---|---|---|---|---|
| [83] | N3-X | Turboelectric | 25 MW | 300 | 4 kV-9 kV | C | 16 |
| [88], [90] | ECO-150 | Turboelectric | 22 MW | 150 | 6 kV | NC | 16 |
| [36] | DC architecture | Turboelectric | 22.4 MW | NA* | 3.6 kV | C | 16 |
| [119] | Raytheon | Turboelectric | 20 MW†† | NA | 2 kV | C | 4 and 8 |
| [94] | DRAGON | Turboelectric | 12.2 MW | 150 | 3 kV (Moderate evolution) | NC | 40 |
| [120] | SynergIE-DEP70 | Turboelectric | $\sim$ 3.5 MW | 70 | 1 kV | NC | 6 and 12 |
| [121] | ULI program | Turbo-hybrid-electric | $\sim$ 16.5 MW | 86 | 2 kV | NC | 8 |
| [122] | LUH Germany | Hybrid-electric | 4 MW | 48 | 3 kV | NC | 6 |
| [123] | The Wright Spirit | Hybrid-electric | 20 MW†† | 100 | 1 kV | NC | 10 |
| [101] | Nottingham, UK | Hybrid-electric | 2 MW | NA | 600 V | NC | 4 |
| [124] | Electric plane with range extender | Hybrid-electric | 723 kW†† | 9 | 400 V | NC | 2+6 |
| [95], [97] | EcoPulse | Hybrid-electric | 350 kW†† | 6 | 800 V | NC | 1+6 |
| [125] | Cryogenic AEA 1 | All-electric | 45 MW†† | NA | 3.3 kV | C | 9 |
| [126] | Cryogenic AEA 2 | All-electric | 40 MW†† | NA | 1 kV | C | 16 |
| [113] | Twin Otter-DEP | All-electric | 990 kW | 19 | 3 kV | NC | 20 |
| [93], [105], [106] | AMPERE | All-electric | 320 kW | 4-6 | 135 V | NC | 40 |
| [52] | X-57 (MOD IV) | All-electric | 240 kW†† | 2 | 461 V | NC | 2+12 |
| [127] | Solar Impulse II | All-electric | 50 kW-Solar†† | 1 | 210 V-304.5 V | NC | 4 |

† Maximum propulsion power required during the mission profile with redundancy considered for one engine inoperative case (unless otherwise specified).
†† Available propulsive power; Not sure about the considered redundancy.
* Not Available.

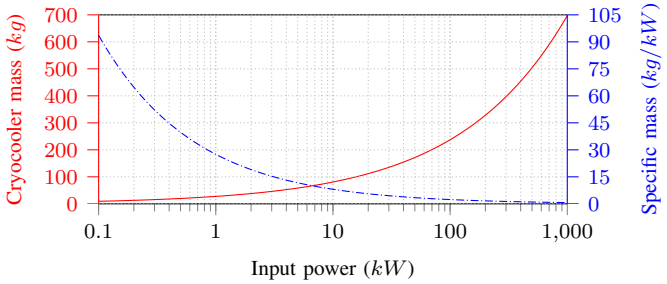


Fig. 23: Variation of cryocooler's mass and specific mass for different input power levels.

$$m_{RBCC} = 27.5 P_{in} e^{-1.225(log_{10} P_{in})} \quad (3)$$

where $m_{RBCC}$ in $kg$ and $P_{in}$ in $kW$ are the mass and input power of the cryocooler, respectively. This equation, which is plotted versus input power in Fig. 23, shows that first, the specific mass of the cryocooler decreases with input power. This means that a decentralized cooling system would result in a higher specific mass and an unacceptable design [65]. Second, the cryocooler mass increases with input power exponentially. Therefore, without significant improvement in motor, generator, and power converter design, the mass of RBCC itself will increase the fuel burn and offset its benefits.

Another challenge with employing cryogenics is that some insulating materials, such as pure polymers, suffer from poor insulating properties at cryogenic temperatures [22]. Furthermore, unlike DC applications, AC superconductors suffer from hysteresis, eddy current, and coupling losses [130]. Hence, even in a DC aircraft power system, the design of the AC superconducting machines is challenging due to the AC losses, and superconductors are only used in the field winding of the machine where a DC current flows. Although NASA has made substantial progress in developing fine-filament magnesium diboride ($MgB_2$) superconductor wire with lower AC losses that can be used in turboelectric aircraft systems, this technology has yet to be incorporated into the power generation or distribution of commercial aircraft [131], [132].

Despite discussed challenges with cryogenic systems, this technology is inevitable in large DEP aircraft. Otherwise, the designed DEP-based large aircraft will not be feasible. For instance, a 150-PAX TeDP aircraft with a 45 MW power rating and 3000 NM mission range was investigated in [133]. The architecture was similar to the one shown in Fig. 4 with 16 thrust-producing distributed propellers. The distribution system voltage of $\pm$270 VDC was adopted. However, the designed power distribution system proved to be so heavy that using current state-of-the-art gravimetric power densities and efficiencies for electric components could not achieve any feasible solution, even after considering unrealistic advancements in power distribution components. Choosing a low voltage of $\pm$270 VDC for such a high-power, non-cryogenic aircraft, which results in an overweight thermal management system, and using a baseline EPS architecture, which is the heaviest architecture in Fig. 15, can be the reasons to justify this infeasible design.

In terms of operating frequency, it has increased from conventional 400 Hz to multiple kHz in recent years [134], [135] due to the high specific power and power density requirements for the electrical apparatus such as electric machines, capacitors, and inductors. This is feasible for multi-MW DEP systems, especially with the advent of commercial high-voltage fast-switching SiC MOSFET modules [136]. The specification of the DEP operating frequency should be determined by comprehensive considerations of the motor rotational speed, power converter efficiency target and switching capability, thermal management and insulation requirements for the major power apparatuses, and the required power density.

In summary, the power conversion system design of single-aisle short-range aircraft diverges significantly from that of the

wide-body long-range ones. The former, which may prefer a non-cryogenic electric propulsion design, necessitates the MVDC power architecture to be adopted in future DEP configurations. However, there are some significant challenges to be addressed in the MVDC systems such as the low PDIV at high altitudes, Corona effect, fault prognosis and protection, surface discharge over different components, and cosmic ray-induced semiconductor failures (which will be discussed in the next section). In particular, a high correlation of design variables in a DEP system, including aerodynamics, electrical, mechanical, and thermal constraints requires multidisciplinary analysis to identify the optimal operating points for the overall system. On the other hand, leveraging the emerging cryogenics and superconductivity technologies to implement a long-range electric propulsion can significantly boost the specific power density and enable low-voltage high-current power conversion system designs. Particularly in a DEP system, in addition to general technological obstacles for cryogenic system and its low TRL, enclosing all distributed propulsors inside a centralized cryocooler or liquid hydrogen tank may introduce new challenges such as a sudden unexpected loss of superconductivity in power apparatuses.

## V. Design Consideration for DEP Power Electronics

As discussed earlier, one of the significant advantages of the DEP is the decoupling between the generator and the motors so that they can operate at their optimal speed. This can be achieved using AC-DC-AC or AC-AC power converters. In addition, to integrate the energy storage components such as batteries and fuel cells into the system, DC-DC converters such as a dual active bridge (DAB) and isolated multiport converters can be utilized to interconnect various energy storage components to the main electric power architecture [137]. Despite a considerable evolution and progress in the field of high-power and high-frequency semiconductor switches [138], designing a high-power converter is still challenging for high-altitude applications. Fortunately, in a DEP, the power rating of electric power converters would be a fraction of the total required power. Additionally, the efficiency, output power quality, modularity, reliability, specific power, and power density of power converters are the critical factors to consider when designing a DEP converter. For the TeDP architectures proposed in [83], it was found that power converters, on average, account for 26.2% of the total system weight (without considering energy storage, fault current limiter, or fuel weight). For the hybrid-electric small concept aircraft discussed in [107], inverters account for 11% of the overall system weight (considering fuel cells, hydrogen tanks, and batteries). Similarly, in an all-electric aircraft, after batteries and fuel cell components, the power converters share a considerable weight of the power system architecture [139].

Voltage source converter (VSC) and current source converter (CSC) are both promising power converter technologies for future distributed propulsion drives. VSC has been widely used and verified in the aviation industry. It has higher efficiency, better input power quality, smaller filter size, and higher reliability compared to CSC [140], [141]. On the other hand, low output-voltage total harmonic distortion (THD) and favorable $dv/dt$, the elimination of the sensitive DC-bus capacitor bank, and the tolerance to DC-bus short-circuit faults make CSC an appropriate option. A challenge with using CSC is that the regular IGBT or MOSFET does not have the reverse-voltage blocking capability and adding a series diode increases the conduction losses [142].

For non-cryogenic aircraft systems, where MVDC is preferred, an inverter with a high specific power of 25 kW/kg and 99% efficiency is envisioned by 2035 [4]. In addition, to drive the high-speed motors of DEP, a high switching frequency of inverter around 20-30 kHz is expected to reduce the size of the passive components and further enhance the specific power. Although high-speed motors may yield lower efficiency due to increased winding AC losses and rotor losses [143], and a gearbox may be required for propeller shaft coupling, high-speed motors generally have high specific power as well, which is favorable for an aircraft. With the high motor speed, the switching frequency of the propulsion inverters should be much higher (e.g., at least 10 times higher than the motor operating frequency). This requires synergistic design optimization of the overall propulsion motor-drive systems to concurrently achieve high efficiency and high power density.

Regarding inverter topologies, SiC-based multilevel inverters are preferred for MVDC applications due to their higher apparent switching frequency, better waveform quality, smaller filter size, higher power density, and use of lower voltage switches [128], [144]. Authors in [145] developed a 1 MW cryogenic-cooled SiC inverter with 1 kV DC-bus voltage by parallel connection of two three-level active neutral point clamped (3L-ANPC) inverters. The efficiency and specific power achieved are 98.5% and 18 kVA/kg, respectively. As will be discussed in Section VI, package considerations restrict the available power modules for high-power applications. Despite their better performance at cryogenic temperatures, available standard Si MOSFETs or GaN devices do not have a suitable package for cryogenic temperatures. On the other hand, a liquid-cooled 1 MW 3L-ANPC inverter with a hybrid utilization of Si and SiC switches based on 2.4 kV DC-bus voltage was developed by General Electric Corporation. A gravitational specific power of 18 kVA/kg and an efficiency of 99.1% were reported [134]. In [146], by using the hybrid switch concept, a modular three-level T-type inverter (100 kW, 1 kV DC bus) was designed. This power electronic building block (PEBB) is estimated to achieve high efficiency of 98.2% and a high specific power of 27.7 kW/kg (excluding the EMI filter).

Another important factor to be considered in designing the power electronic for aircraft applications is their reliability and ruggedness against cosmic radiation-induced semiconductor failures. Cosmic-ray shower, which causes single-event burnout (SEB) and single-event gate rupture (SEGR) failures, is of random type and hence, is not time-dependent. Terrestrial neutrons can potentially cause permanent damage to power semiconductors in high-voltage blocking states. To be specific, the cosmic-ray-induced failure rate is a function of the DC-bus voltage, the device junction temperature, and the flight

altitude, as shown in the equation below [147]:

$$\lambda(V_{DC}, T_j, h) = \left[C_3 \cdot exp\left(\frac{C_2}{C_1 - V_{DC}}\right)\right] \cdot exp\left(\frac{25 - T_j}{47.6}\right) \cdot exp\left(\frac{1 - (1 - \frac{h}{44300})^{5.26}}{0.143}\right) \quad (4)$$

where $\lambda$ is the failure rate of the power switch in FIT, that is, the number of failures within $10^9$ element hours. $C_1, C_2$, and $C_3$ are device-specific constants without physical meaning, DC-bus voltage $V_{DC}$ is the voltage across the switch, $T_j$ is the junction temperature in Celsius, and $h$ is the height above sea-level in meters. As can be seen, the higher the altitude, the higher the failure rate of the power semiconductor switches subject to cosmic radiation. Therefore, compared with the sea-level condition, a greater safety margin should be considered in the blocking voltage and junction temperature of the power switches to decrease the probability of SEB or SEGR failures at cruising altitudes [128].

It should be noted that the area-normalized FIT values do not change considerably with the rated voltage of the device as long as the ratio of (*bias voltage*)/(*breakdown voltage*) is kept constant. In other words, to design an inverter for DEP considering the cosmic ray reliability, that is the ratio of the applied voltage to the avalanche (breakdown) voltage which is important not the rated voltage of the device [150]. Furthermore, SiC devices, including both MOSFETs and diodes, have been found more robust and significantly rugged against cosmic radiations compared to Si IGBTs and diodes in the high-bias ranges [151], [152]. From this point of view, SiC devices are recommended for high-voltage aerospace applications.

Besides efficiency, power density, specific power, and reliability, the modular design of the power converter is also of great importance. Using low voltage and low current submodules in a modular multilevel converter (MMC) enables high power conversion at very high voltages and reduces the maintenance time and manufacturing complexity [153].

A future challenge for power electronics engineers in aviation industries could be developing an integrated motor drive (IMD) system, which is basically a structural combination of the power electronic converter and the electric motor as a single unit. In [148], a 1 MW IMD with a DC-bus voltage of 2 kV and six modular inverters mounted on the circumferential surface of the motor was designed, as shown in Fig. 24. An active gravimetric specific power and efficiency of 23.7 kW/kg and 97.2%, respectively, are predicted for the machine part of this IMD design [121]. IMD can improve the volumetric power density by 10-20% and reduce system costs by 30-40% [154]. It would eliminate the need for separate housings, high voltage bus bars, and more importantly, long cables between the inverter and the motor which cause high EMI and overvoltages across motor stator windings at high switching speeds [128], [154]. However, such integration technologies can present challenges to thermal management and mechanical design, especially at high-altitude operating conditions. The power converter would be exposed to the high temperature of the motor, thermal cycling, and vibrations caused by the motor [149]. The use of wide bandgap devices in IMDs will mitigate the challenges, as they have smaller footprint and higher limit for high-temperature operation [155], [156]. All these challenges must to be considered in the multi-physics system design optimization to ensure high reliability of the power converters in harsh working environments.

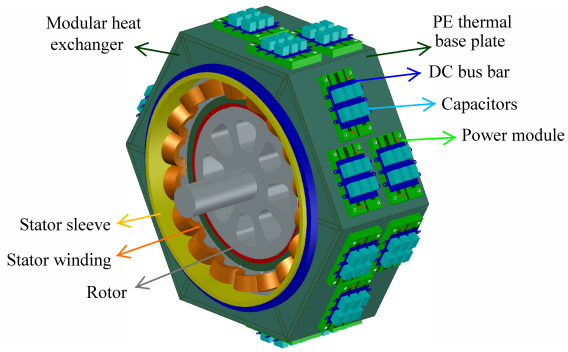


Fig. 24: Integrated motor drive concept with six modular inverters mounted around the motor. Each inverter drives a set of three-phase winding [148], [149].

In conclusion, since there are multifarious power converter technologies available with different characteristics, a point-by-point comparison is required to select the optimal circuit topology considering specific design requirements and mission profiles. To this end, a model-based synergistic co-design modeling and simulation would be necessary to evaluate power losses, thermal, power density, and electrical reliability with a typical mission profile [157], [158]. As indicated from a list of high-power medium-voltage aircraft propulsion drives in Table IV, employing SiC-based multilevel converters enables a highly efficient and compact electrical design of the propulsion drive systems.

Meanwhile, the power converters should be evaluated based on reliability characteristics such as fault tolerance and reliability against cosmic-ray failure at high altitude, EMI, dielectric insulation derating at low air pressure, etc. The high $dv/dt$ produced from the high-frequency SiC converters is also challenging for DEPs, since it may cause significant reflected voltage spikes and bearing currents on the motor side, if an effective filtering solution is unavailable. In a DEP system, the propulsion motors have lower horsepower but higher surge impedance, leading to more severe surge impedance mismatch between the cables and motors. Hence, they might be more susceptible to surge voltage stresses across the stator

TABLE IV: High-power, medium-voltage inverters proposed for aircraft applications.

| Ref. | Inverter type | Feature | Power level | Voltage level | Specific power (kW/kg) | Efficiency |
|---|---|---|---|---|---|---|
| [134] | 3L-ANPC | Hybrid Si+SiC inverter | 1 MW | 2.4 kV | 18 | 99.1% |
| [146] | T-type PEBB | Hybrid Si+SiC switch | 0.1 MW | 1 kV | 27.7† (predicted) | 98.2% |
| [145] | Parallel 3L-ANPC | Cryogenic All-SiC | 2× 0.5MW | 1 kV | 18 | 98.5% |
| [148] | 2-level | IMD | 1 MW | 2 kV | 23.7†† (predicted) | 97.2†† % (predicted) |

† 24.5 kW/kg with EMI filter.
†† Considering only the machine part.

windings and insulation degradation, especially at high altitude low-pressure conditions [159]. Therefore, assuming that the thermal management and mechanical vibration challenges with IMDs can be overcome, multilevel WBG-based IMD converters would be an attractive propulsion solution for implementing the DEP configurations.

## VI. Cryogenic conditions for DEP power electronics

To achieve high power density and efficiency, a superconducting system has been proposed for large twin-aisle aircraft, as can be seen in Table III. Using a cryogenic system can significantly reduce ohmic losses and improve the systematic power density. In addition to superconducting electric machines [160], [161], cables [162], and circuit breakers [163], power converters [164] will also be operating at cryogenic temperatures, requiring thorough investigations for safe and effective integration of electrical and cooling systems. Considering the specific mission profile of aircraft applications, a flexible power rating of superconducting devices was proposed in [165]. Based on this concept, during climb or device failures when high power is required, the flow rate of the cryogen is increased to lower the temperature and increase the power rating. This would reduce the redundancy requirement of the system. However, synergistic co-designs between the thermal and electrical domains are needed.

Major challenges of developing cryogenic DEP systems include achieving a high coefficient of performance (COP) for the cryocooler, dealing with AC losses and developing a fully superconducting motor, managing high magnitudes of the fault currents due to DC capacitive discharge and low resistance of the entire system [129], [162], and handling the high heat load of power converters [166]. For power converters, which use semiconductors and passive devices, the behavior of the components at cryogenic temperatures will be briefly discussed here.

As discussed in Section V, the advantages of high operating frequency, high specific power and power density, and enhanced efficiency can be achieved by employing wide bandgap devices in DEP systems. However, the power semiconductors' behavior at cryogenic temperature varies from that at room temperature. The on-state resistance, switching losses, avalanche ruggedness, and breakdown voltage are the key parameters of interest that change with the temperature [167]–[174]. The variation of specific on-state resistance ($R_{on,sp}$) with temperature for Si MOSFET, SiC MOSFET, and Gallium Nitride (GaN) transistors are shown in Fig. 25a [168]. It can be seen that as the temperature is reduced and it approaches 77 K, the $R_{on,sp}$ of the GaN device decreases fivefold. However, Si and SiC MOSFETs show different behaviors. The $R_{on,sp}$ of SiC devices increases by 1.5 to 3.5 times as the temperature decreases to 77 K. The Si MOSFETs first experience a sharp reduction of $R_{on,sp}$ until the temperature reaches around 100 K, and then it begins to increase again due to carrier freeze-out [168]. Fig. 25b also depicts that the breakdown voltage for Si devices is reduced by around 300 V on average, while that of the SiC and GaN devices is relatively unchanged.

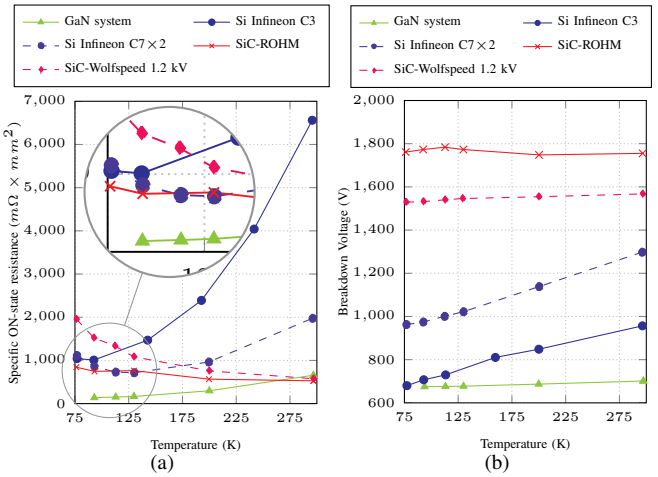


Fig. 25: Comparison of the Si, SiC, and GaN devices (a) specific on-state resistance variation with temperature, and (b) breakdown voltage variation with temperature [168].

Therefore, a larger voltage margin should be considered for Si devices at the cryogenic condition than that at the room temperature.

Switching loss variations versus temperature for a SiC-MOSFET and a Si-IGBT, both rated at 1.2 kV, as well as a 650 V GaN device, are shown in Fig. 26 [172], [175]. The turn-on and turn-off losses of the IGBT reduce considerably and continuously as the temperature drops from 493 K to 90 K, while the turn-on energy reduction is around threefold compared with that of the turn-off process. The lower switching energy at cryogenic temperature is mainly due to the shorter lifetime of the minority carriers, and, consequently, faster carrier modulation (during turn-on) and carrier recombination (during turn-off) processes [172]. On the other hand, the turn-on switching energy of the SiC MOSFET first increases and then decreases as the temperature drops to and below 170 K, respectively. The turn-off energy of the SiC remains almost unchanged as the temperature decreases. Accordingly, the switching losses of the IGBT become comparable with those of the SiC MOSFET at cryogenic temperatures. Therefore, considering only switching losses, SiC MOSFETs are

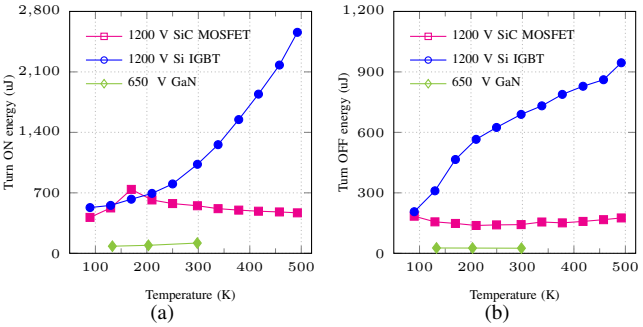


Fig. 26: Comparison of the switching losses variation versus temperature for different switching devices (a) Turn-on energy, and (b) Turn-off energy; (Condition for IGBT and SiC: $V_{DD}$=800 V, $I_{DS}$=20 A, $R_g$=3.33 Ω [172], and condition for GaN: $V_{DD}$=400 V, $I_{DS}$=20 A, $R_{gON}$=20 Ω, $R_{gOFF}$=2 Ω [175]).

superior only at the room temperature. For the GaN switch, it should be noted that the test condition i.e., voltage and gate resistance, is different from the other devices. While its turn-on loss decreases at lower temperatures, turn-off loss increases moderately. Therefore, the total switching loss slightly reduces as the temperature drops from 298 K to 133 K.

Avalanche capabilities were compared among planar/trench SiC MOSFETs and Si IGBT in [174]. It was concluded that cryogenic temperature would enhance the avalanche energy density of all devices, and generally SiC devices have higher avalanche energy than Si IGBT over the temperature range of 90 K to 340 K.

Another challenge in designing power converters for cryogenics is the semiconductor package degradation at low temperatures. Although discrete semiconductor devices may not degrade at cryogenic temperatures [176], large power modules are susceptible to failure [177]. Different coefficients of thermal expansion (CTE) for solder joints, wire bonds, and silicon gel in a power module can potentially cause device failure. Hence, Press-Pack IGBTs or IGCTs are suggested in [177] for cryogenic applications, and converter topologies like current source converters or direct converters are recommended to eliminate or minimize the vulnerable DC capacitor bank of the converter.

The general performance comparison in cryogenics among different switches is summarized in Fig. 27 [178]. Accordingly, the Si MOSFET and GaN devices have, respectively, the lowest on-state resistance and switching losses at cryogenics compared with the others. Despite its improved performance at cryogenic temperatures, IGBT is still difficult to use at switching frequencies over 1 kHz. Using Si MOSFET in [178], a 40 kW, three-level ANPC inverter was developed for cryogenic temperature, and with 97.8% efficiency, the loss was reportedly lowered by 30%, compared with the scenario at room temperature.

For passive components, including inductors and capacitors, comparative studies have been reported in [179]–[181]. Ferrite and amorphous cores are not recommended for cryogenic temperatures because of their high loss and low permeability. Although nanocrystalline cores are expensive, and their loss slightly increases at cryogenic temperatures, they can be useful at cryogenic temperatures because of their relatively higher permeability and lower loss compared to that of amorphous and ferrite. Among film capacitors, polypropylene and polyphenylene sulfide are preferred because, unlike polyester or polycarbonate with decreasing capacitance at low temperatures, they have almost constant capacitance at room and cryogenic temperatures. Furthermore, tantalum capacitors are better than electrolytic ones at cryogenic temperatures due to the significant decrease in capacitance in electrolytic types [181].

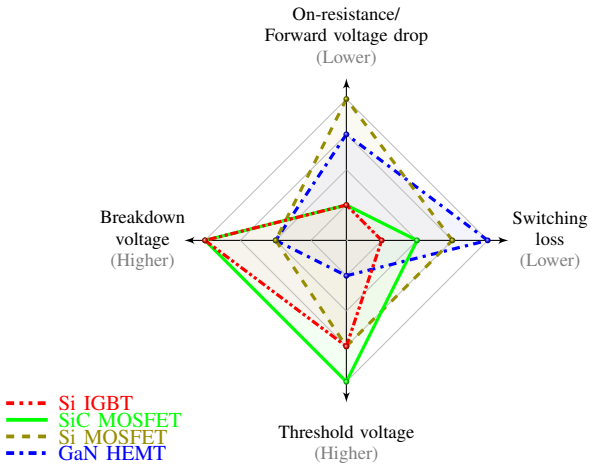


Fig. 27: Performance comparison among Si IGBT, Si MOSFET, SiC MOSFET, and GaN HEMT at a cryogenic temperature [178].

## VII. Energy Storage for DEP

Distributed energy storage is another critical subsystem in DEPs that determines the payload capacity and flight range of the HEA or AEA. Due to the low technology readiness levels (TRL) of the energy storage components, intensive research studies are required to assess their impact on DEP systems. Although DEP does not need energy storage to enable BLI, lower fan pressure ratio (FPR) fuel burn saving, and Gg $CO_2$ equivalents reduction, energy storage brings further fuel burn saving and emission reduction. However, the increased powertrain mass of batteries and motors, particularly in single-aisle HEA and AEA, may offset the potential benefits of the DEP. A comparison between 150-PAX hybrid distributed electric propulsion (HDEP) and the boosted turbofan configurations in [182] shows that the propulsion mass of the designed HDEP is around 6-7 times higher than that of the boosted turbofan and baseline architectures.

Different energy storage components have different performances in terms of energy density, power density, specific power, lifetime, and cost. As shown in Fig. 28, hydrogen-based fuel cells have much higher gravimetric and volumetric energy densities than supercapacitors and batteries, while supercapacitors have higher specific power and faster charging and discharging speed than fuel cells and batteries [24]. Although, Silicon Nanowire Anode-based Li-ion battery cells were recently reported to achieve 1.2 kWh/L at 450 Wh/kg [183], the typical volumetric energy density for Li-ion batteries is around 400 Wh/L, which is much lower than the 2.5 kWh/L of the Liquid Hydrogen ($LH_2$)-based Fuels. Biofuel-based fuel cells with higher Wh/L, Wh/kg, and boiling point temperatures can also be used to increase the aircraft range and payload.

For small electric aircraft up to a few megawatts, using distributed batteries or a hybrid combination of both batteries and supercapacitors is feasible to meet the general power requirements. Although the weight and energy density of the batteries used in electric vehicles (EVs) or electric ships are used as a reference to predict the battery requirement of future AEA [35], it should be noted that design considerations are different in AEA applications. Higher safety, faster charging and discharging rate, longer peak-power duration, and more complicated thermal management strategies are required to avoid the thermal runaway of batteries in an AEA.

A DEP system with a hybrid storage consisting of batteries and supercapacitors was proposed in [186] for X-57 *Maxwell*

This article has been accepted for publication in IEEE Transactions on Transportation Electrification. This is the author's version which has not been fully edited and content may change prior to final publication. Citation information: DOI 10.1109/TTE.2022.3197332



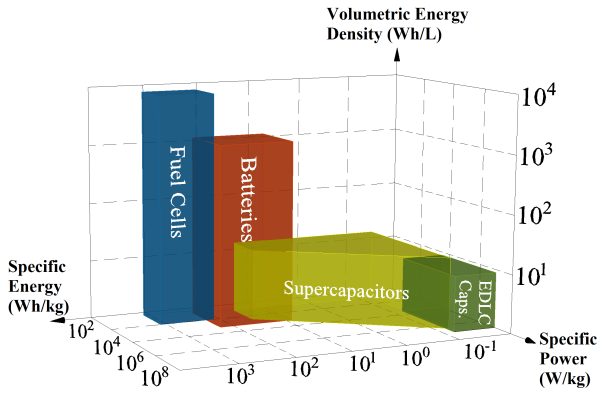


Fig. 28: Comparison of various ESS components [24], [183]–[185].

Mod II. Compared to the normal battery-based system, weight and volume reductions of 21.5% and 17.4%, respectively, were reported for the hybrid system. The existing energy density of batteries limits the payload and range of the AEA to 20 PAX and 600 NM, respectively. An AEA with hybrid energy sources of lightweight solid-oxide fuel cell (SOFC), gas turbine, and battery (FC-GT-B) was proposed in [187] to achieve maximum payload and to be comparable with existing gas turbine-based aircraft. High energy density of $LH_2$ and high efficiency of SOFC countervailed the increased weight of the power system and, ultimately, power and energy densities of 0.9 kW/kg and 7 kWh/kg, respectively, were reported for that FC-GT-B concept.

For large wide-body airplanes, using distributed fuel cells may be promising due to high energy density and the absence of carbon emissions, while combinations with supercapacitors or batteries may be beneficial to improve the power demand response onboard. A concept design of a propulsion system using a hydrogen fuel cell and battery with superconducting motors was presented in [125]. The battery was mainly used for the takeoff and climb-out phases of the mission profile when there was a high power demand. The results show that the hybrid system still has yet to achieve the same specific power as the Airbus A320. It could be possible when the specific energy densities of the battery and liquid hydrogen system reach 8 kWh/kg and 3.7 kWh/kg, respectively, but this goal may take several decades.

The maximum efficiency of modern proton exchange membrane fuel cells is reported to be around 60 to 70% [188], but generally, fuel cells have efficiencies of around 50-60% and most of the loss is released as heat. Hence, effective cooling should be considered for high-power installations. In [103], [104], a feasibility study for electrifying the aircraft model De Havilland Canada Dash 8 (DH8D) was investigated by replacing the maximum fuel capacity of conventional Kerosene with a fuel cell and batteries. Aircraft range can be calculated using (5), for the cases where fuel cell or kerosene is used, and (6), for the case of using batteries as energy storage [103].

$$R_1 = E^* \cdot \eta_{total} \cdot \frac{1}{g} \cdot \frac{L}{D} \cdot ln(\frac{1}{1-\frac{m_{fuel}}{m}}) \tag{5}$$

$$R_2 = E^* \cdot \eta_{total} \cdot \frac{1}{g} \cdot \frac{L}{D} \cdot \frac{m_{battery}}{m} \tag{6}$$

Where $E^*$ is the energy density of the corresponding fuel, $\eta_{total}$ is the total efficiency of the system, $g$ is the standard gravity, and $\frac{L}{D}$ is the lift to drag ratio. In addition, $m$, $m_{battery}$, and $m_{fuel}$ are respectively the total mass, the battery mass, and the kerosene/hydrogen mass. The study results revealed that the all-electric aircraft, regardless of the type of energy storage used (fuel cell, battery, supercapacitor, or hybrid), is not competitive with the conventional aircraft, neither in flight range nor payload capacity. However, future improvements in the specific power of energy storage could make AEA competitive with the conventional aircraft.

Using hybrid energy storage also creates the opportunity for optimal power management in DEPs. Specifically, a low-pass filter can be used to decouple the low- and high-frequency voltage components. Then, the supercapacitor and battery can be managed to respond to high- and low-frequency fluctuations of DC-bus voltage, respectively. Thus, increased battery lifetime, improved dynamic response of the system, and optimized sizing will be realized in this way [189]. The high cost of the supercapacitor and additional power electronic interfaces are the main drawbacks of this hybrid energy storage approach.

Energy storage can also improve system stability and fault tolerance in hybrid DEP configurations. It can reduce the failure impacts and mitigate the system collapse if one of the engines or generators fails [98], [190]. Although batteries or superconducting magnetic energy storage units are not deployed for propulsion purposes in the normal mode of the TeDP system, they can increase the system survivability following a generator loss and system reconfiguration. In [190], Li-ion battery storage is used to prevent voltage collapse by mitigating overload conditions, injecting power, and helping the remaining healthy generators to come out from the stalling zone. However, there are challenges with battery weight and response time required for such an operation. Here, the minimum required power ($P_{ess}^{min}$) and maximum time ($T_{ess}^{max}$) for the energy storage system (ESS) to turn on and start stabilizing the system can be calculated as follows [190]:

$$P_{ess}^{min} = P_L - \tau_m^{max} \frac{V_{g,lim}}{\sqrt{3}K_e} \tag{7}$$

$$T_{ess}^{max} = (\frac{V_{g,lim}^2}{3K_e^2\omega_o^2} - 1)(\frac{H}{\Delta P_{pu}}) \tag{8}$$

where $P_L$ and $\tau_m^{max}$ are the load power and maximum mechanical torque of the prime mover, respectively. $V_{g,lim}$ is the low-voltage limit of the generator terminal, and $K_e$ is the back electromotive force (EMF) constant. Furthermore, $\omega_o$, $H$, and $\Delta P_{pu}$ are the synchronous speed, inertia constant, and load change in $pu$, respectively. Basically, the right side of the equation (7) is the power mismatch between load and prime mover, which should be supplied by ESS. Furthermore, the higher the load change, $\Delta P_{pu}$, the faster the generator terminal voltage will drop and the shorter the $T_{ess}^{max}$ will become. Therefore, those architectures with lower interconnections and less number of sources on buses will suffer more from larger

TABLE V: Comparison of aircraft systems with different energy storage systems.

| Ref. | Energy source | Baseline | Achievement | Drawback compared to the baseline |
|---|---|---|---|---|
| [186] | **All electric**<br>- Battery<br>- Supercapacitor | Battery-electric X-57 Mod II | - Weight reduction of 21%<br>- Volume reduction of 17.4% | - Complexity<br>- Expensive supercapacitor |
| [187] | **All electric**<br>- SOFC<br>- Battery | 4 existing gas turbine aircraft | - Specific power of 0.9 kW/kg<br>- Energy density of 7 kWh/kg | Complexity |
| [125] | **All electric**<br>- $LH_2$ fuel cell<br>- Battery | Airbus A320 | Specific power of 6.25 kW/kg | - Low Specific power<br>- Needs superconductive motors |
| [104]<br>[103] | **All electric**<br>- Fuel cell<br>- Battery | Range of DH8D | Max. range of 987.5 km & 427.5 km for fuel cell & battery systems, respectively | Much lower range and payload |
| [189] | **Hybrid electric**<br>- Fuel<br>- Battery<br>- Supercapacitor | Non-optimized hybrid ESS | - Increased battery lifetime<br>- Improved dynamic response<br>- Optimized sizing | - Complexity<br>- Added converter for supercapacitors<br>- Costly |
| [98] | **Hybrid electric**<br>- Fuel<br>- Battery | Conventional fuel-based aircraft | - Same performance ($\frac{payload \times range}{energy\ consumed}$) as the baseline<br>- Improved fault-tolerance | - Limited range<br>- Assumed power densities are not available yet |
| [190] | **Turboelectric**<br>- Fuel<br>- Battery as ESS | Turboelectric Without ESS | - System survivability after a generator failure | - Extra batteries<br>- Extra inverters<br>- Added mass |

required ESS power and short survival time after a fault and EPS reconfiguration.

DEP projects using ESS in the literature are summarized in Table V. Accordingly, hybrid ESS is aimed to maximize the advantages, and future improvements in the power and energy densities as well as the specific power of ESS is required to make them feasible.

## VIII. Future trends

Future trends and research focus in electrified aircraft, and particularly in DEP systems can be summarized as follows:

- Starting with EPS, integration of fault protection and power conversion components in single lightweight units, as well as higher voltage levels, are expected to considerably reduce the system weight and complexity. This indeed requires advanced insulation material with high relative permittivity and dedicated design consideration to prevent partial discharging at high altitudes.
- In cryogenic power conversion systems, advanced high-efficiency AC superconductors can dramatically optimize the EPS architecture and reduce the motor winding losses.
- High-voltage (3.3 kV and above), high-frequency SiC semiconductor switches are not mature enough to meet aviation reliability standards, and these high-voltage SiC switches typically exhibit high switching losses at high switching frequencies. In addition, power module packaging improvement is a requisite for cryogenic applications.
- Intensive research is needed to enhance the overall power density and reliability of the propulsion drivetrain systems using the IMD designs. This requires multi-physics investigations to address the challenges of mechanical vibration/noise, thermal management, and mechanics.
- There is proactive research in the literature aimed at retrofitting hybrid energy storage systems into existing aircraft electrical architectures. Considering the specific mission profile of aircraft, hybrid energy storage systems can be utilized to increase the aircraft range and meet the high- and low-frequency power demand of electric propulsion.
- $LH_2$, either used in fuel-cells or in hydrogen-powered aircraft engines, has the potential to be the fuel of future aviation, provided the challenges with the production process, lower volumetric density, aircraft redesign to comprise large $H_2$ tanks, and safety issues are overcome. $LH_2$ is the most probable and practical alternative for kerosene, as it contains higher energy per kilogram, zero $CO_2$, and much less nitrogen oxide emission.
- Due to the EPS complexity and harsh operating environment, novel online health monitoring and prognostics techniques such as digital reliability twin technologies are required to predict the remaining lifetime of DEP systems.
- Last but not least, certifying challenges and safety assessment standards need to be addressed by aviation administrators. As a disruptive technology, DEP has unconventional designs in all aerodynamic, mechanical, and electrical domains. Therefore, specific standards and regulations are of paramount importance to evaluate a DEP system in different stages of the design process.

## IX. Conclusion

This paper presents a comprehensive review of the emerging distributed electric propulsion technologies for three various propulsion architectures: turboelectric, hybrid-electric, and all-electric propulsion systems. The performance advantages of the DEP systems are summarized, and the existing DEP design examples in the literature are compared. As vital components of the DEP, several power distribution architectures, which can significantly affect the system weight, performance, and even feasibility, are reviewed. Afterward, parametric specifications of the DEP architectures and the state-of-the-art high-power converters are discussed with an emphasis on the significance of the MVDC in future aircraft. The medium-voltage, high-power, integrated motor drive technologies can improve the combined power density of the future propulsion powertrains. Since implementing DEP in large aircraft (with tens of megawatts of power rating) would be more feasible using a cryogenic system, the characteristics of power electronic components operating at cryogenic temperature conditions are also presented. Finally, various energy storage components are reviewed for DEP systems which can potentially provide further fuel saving and $CO_2$ abatement. The low specific power of state-of-the-art batteries is the main barrier to the implementation of HEA and AEA. This can be overcome by using other types of energy storage units such as fuel cells.

This review of the state of the art of aircraft DEP technologies aims to provide a comprehensive reference for researchers and engineers, as well as policy and standard makers in the aviation and aerospace domains, in order to accelerate the DEP development, along with the research and development (R&D) of green fuel such as green hydrogen or supercritical $CO_2$ ($sCO_2$) and its potential gigagram $CO_2$ equivalent elimination—with or without combustion, for future net-zero emission flight.

## Acknowledgment

This work is based upon work supported in part by the U.S. National Science Foundation (NSF) under Award 2135543, and in part by the U.S. NSF Award ECCS-2146350.

## REFERENCES


[1] V. Madonna, P. Giangrande, and M. Galea, "Electrical power generation in aircraft: Review, challenges, and opportunities," *IEEE Trans. on Transportation Electrification*, vol. 4, no. 3, pp. 646–659, 2018.

[2] J. Bourdon, P. Asfaux, and A. M. Etayo, "Review of power electronics opportunities to integrate in the more electrical aircraft," in *2015 international Conf. on electrical systems for aircraft, railway, ship propulsion and road vehicles (ESARS)*. IEEE, 2015, pp. 1–6.

[3] I. Moir, A. Seabridge, and M. Jukes, *Civil avionics systems*. John Wiley & Sons, 2013.

[4] T. C. Cano, I. Castro, A. Rodríguez, D. G. Lamar, Y. F. Khalil, L. Albiol-Tendillo, and P. Kshirsagar, "Future of electrical aircraft energy power systems: An architecture review," *IEEE Trans. on Transportation Electrification*, vol. 7, no. 3, pp. 1915–1929, 2021.

[5] "Net-zero carbon emissions by 2050," [Online], October 2021, https://www.iata.org/en/pressroom/2021-releases/2021-10-04-03/ (accessed Aug. 3,2022).

[6] R. L. Speth, S. D. Eastham, T. M. Fritz, I. Sanz-Morere, A. Agarwal, P. Prashanth, F. Allroggen, and S. R. Barrett, "Global environmental impact of supersonic cruise aircraft in the stratosphere," NASA Technical Reports, 2021.

[7] X. Roboam, B. Sareni, and A. De Andrade, "More electricity in the air: Toward optimized electrical networks embedded in more-electrical aircraft," *IEEE industrial electronics magazine*, vol. 6, no. 4, pp. 6–17, 2012.

[8] "Have noise levels changed over the years?" [Online], available: https://noise.flysfo.com/2019/09/30/have-noise-levels-changed-over-the-years/.

[9] "Noise data for the first 17 months of boeing 787 operations at Heathrow airport," *Civil Aviation Authority*, Technical report, 2014.

[10] "Noise data for the first three years of airbus a350 operations at Heathrow airport," *Civil Aviation Authority*, Technical report, 2019.

[11] D. L. Huff *et al.*, "Noise reduction technologies for turbofan engines," *National Aeronautics and Space Administration*, 2007.

[12] L. Shang, G. Liu, and P. Hodal, "Development of high performance aircraft bleed air temperature control system with reduced ram air usage," *IEEE Trans. on control systems technology*, vol. 18, no. 2, pp. 438–445, 2009.

[13] G. Qiao, G. Liu, Z. Shi, Y. Wang, S. Ma, and T. C. Lim, "A review of electromechanical actuators for more/all electric aircraft systems," *Proceedings of the Institution of Mechanical Engineers, Part C: Journal of Mechanical Engineering Science*, vol. 232, no. 22, pp. 4128–4151, 2018.

[14] H. D. Kim, A. T. Perry, and P. J. Ansell, "A review of distributed electric propulsion concepts for air vehicle technology," in *2018 AIAA/IEEE Electric Aircraft Technologies Symposium (EATS)*. IEEE, 2018, pp. 1–21.

[15] P. F. Pelz, P. Leise, and M. Meck, "Sustainable aircraft design—a review on optimization methods for electric propulsion with derived optimal number of propulsors," *Progress in Aerospace Sciences*, vol. 123, p. 100714, 2021.

[16] A. S. Gohardani, G. Doulgeris, and R. Singh, "Challenges of future aircraft propulsion: A review of distributed propulsion technology and its potential application for the all electric commercial aircraft," *Progress in Aerospace Sciences*, vol. 47, no. 5, pp. 369–391, 2011.

[17] M. Burston, K. Ranasinghe, A. Gardi, V. Parezanovic, R. Ajaj, and R. Sabatini, "Design principles and digital control of advanced distributed propulsion systems," *Energy*, p. 122788, 2021.

[18] K. Davies, P. Norman, C. Jones, S. Galloway, and M. Husband, "A review of turboelectric distributed propulsion technologies for N+3 aircraft electrical systems," in *2013 48th International Universities' Power Engineering Conf. (UPEC)*. IEEE, 2013, pp. 1–5.

[19] J. Z. Bird, "A review of electric aircraft drivetrain motor technology," *IEEE Trans. on Magnetics*, vol. 58, no. 2, pp. 1–8, 2021.

[20] Z. Huang, T. Yang, P. Giangrande, M. Galea, and P. Wheeler, "Technical review of dual inverter topologies for more electric aircraft applications," *IEEE Trans. on Transportation Electrification*, 2021.

[21] E. Sayed, M. Abdalmagid, G. Pietrini, N.-M. Sa'adeh, A. D. Callegaro, C. Goldstein, and A. Emadi, "Review of electric machines in more-/hybrid-/turbo-electric aircraft," *IEEE Trans. on Transportation Electrification*, vol. 7, no. 4, pp. 2976–3005, 2021.

[22] M. Borghei and M. Ghassemi, "Insulation materials and systems for more and all-electric aircraft: A review identifying challenges and future research needs," *IEEE Trans. on Transportation Electrification*, 2021.

[23] A. Bakhshi, M. Bigdeli, M. Moradlou, and H. M. CheshmehBeigi, "More electric aircraft fault current protection: A review," in *2021 12th Power Electronics, Drive Systems, and Technologies Conf. (PEDSTC)*. IEEE, 2021, pp. 1–7.

[24] J. Benzaquen, J. He, and B. Mirafzal, "Toward more electric powertrains in aircraft: Technical challenges and advancements," *CES Trans. on Electrical Machines and Systems*, vol. 5, no. 3, pp. 177–193, 2021.

[25] C. Dong, Y. Qian, Y. Zhang, and W. Zhuge, "A review of thermal designs for improving power density in electrical machines," *IEEE Trans. on Transportation Electrification*, vol. 6, no. 4, pp. 1386–1400, 2020.

[26] L. Dorn-Gomba, J. Ramoul, J. Reimers, and A. Emadi, "Power electronic converters in electric aircraft: current status, challenges, and emerging technologies," *IEEE Trans. on Transportation Electrification*, vol. 6, no. 4, pp. 1648–1664, 2020.

[27] A. Barzkar and M. Ghassemi, "Electric power systems in more and all electric aircraft: A review," *IEEE Access*, vol. 8, pp. 169 314–169 332, 2020.

[28] K. Ni, Y. Liu, Z. Mei, T. Wu, Y. Hu, H. Wen, and Y. Wang, "Electrical and electronic technologies in more-electric aircraft: A review," *IEEE Access*, vol. 7, pp. 76 145–76 166, 2019.

[29] G. Buticchi, S. Bozhko, M. Liserre, P. Wheeler, and K. Al-Haddad, "On-board microgrids for the more electric aircraft—technology review," *IEEE Trans. on Industrial Electronics*, vol. 66, no. 7, pp. 5588–5599, 2018.

[30] J. Chen, C. Wang, and J. Chen, "Investigation on the selection of electric power system architecture for future more electric aircraft," *IEEE Trans. on Transportation Electrification*, vol. 4, no. 2, pp. 563–576, 2018.

[31] R. C. Bolam, Y. Vagapov, and A. Anuchin, "Review of electrically powered propulsion for aircraft," in *2018 53rd international universities power engineering Conf. (UPEC)*. IEEE, 2018, pp. 1–6.

[32] X. Zhao, J. M. Guerrero, and X. Wu, "Review of aircraft electric power systems and architectures," in *2014 IEEE International Energy Conf. (ENERGYCON)*. IEEE, 2014, pp. 949–953.

[33] B. Sarlioglu and C. T. Morris, "More electric aircraft: Review, challenges, and opportunities for commercial transport aircraft," *IEEE Trans. on Transportation Electrification*, vol. 1, no. 1, pp. 54–64, 2015.

[34] B. Rahrovi and M. Ehsani, "A review of the more electric aircraft power electronics," in *2019 IEEE Texas Power and Energy Conf. (TPEC)*. IEEE, 2019, pp. 1–6.

[35] R. Alexander, D. Meyer, and J. Wang, "A comparison of electric vehicle power systems to predict architectures, voltage levels, power requirements, and load characteristics of the future all-electric aircraft," in *2018 IEEE Transportation Electrification Conf. and Expo (ITEC)*. IEEE, 2018, pp. 194–200.

[36] C. E. Jones, P. J. Norman, S. J. Galloway, M. J. Armstrong, and A. M. Bollman, "Comparison of candidate architectures for future distributed propulsion aircraft," *IEEE Trans. on applied superconductivity*, vol. 26, no. 6, pp. 1–9, 2016.

[37] M. A. Rendón, J. Gallo, A. H. Anzai *et al.*, "Aircraft hybrid-electric propulsion: Development trends, challenges and opportunities," *Journal of Control, Automation and Electrical Systems*, pp. 1–25, 2021.

[38] R. Bojoi, L. Boggero, S. Comino, M. Fioriti, A. Tenconi, and S. Vaschetto, "Multiphase drives for hybrid-electric propulsion in light aircrafts: a viable solution," in *2018 International Symposium on Power Electronics, Electrical Drives, Automation and Motion (SPEEDAM)*. IEEE, 2018, pp. 613–619.

[39] "Hydrogen, an important pathway to our zero-emission ambition," https://www.airbus.com/en/innovation/zero-emission/hydrogen (accessed Aug. 3,2022).

[40] "GE aviation and Safran launch advanced technology demonstration program for sustainable engines; extend CFM partnership to 2050," https://www.geaviation.com/press-release/other-news-information/ge-aviation-and-safran-launch-advanced-technology (accessed Aug. 3,2022).

[41] "COP26 goals, what do we need to achieve at COP26?" https://ukcop26.org/cop26-goals/ (accessed Aug. 3,2022).

[42] A. Dianov, F. Tinazzi, S. Calligaro, and S. Bolognani, "Review and classification of MTPA control algorithms for synchronous motors," *IEEE Trans. on Power Electronics*, 2021.

[43] S. Sakunthala, R. Kiranmayi, and P. N. Mandadi, "A review on speed control of permanent magnet synchronous motor drive using different control techniques," in *2018 International Conf. on Power, Energy, Control and Transmission Systems*. IEEE, 2018, pp. 97–102.

[44] D. L. Simon, "System-level control concepts for electrified aircraft propulsion systems," NASA Technical Reports, 2022.

[45] R. C. Bolam, Y. Vagapov, and A. Anuchin, "A review of electrical motor topologies for aircraft propulsion," in *2020 55th International Universities Power Engineering Conf. (UPEC)*. IEEE, 2020, pp. 1–6.

[46] Z. Wang, Z. Lv, P. Yu, Z. Li, and B. Wang, "Research status of high temperature superconducting power cable," in *2022 IEEE International Conf. on Electrical Engineering, Big Data and Algorithms (EEBDA)*. IEEE, 2022, pp. 182–186.

[47] X. Pei, O. Cwikowski, D. S. Vilchis-Rodriguez, M. Barnes, A. C. Smith, and R. Shuttleworth, "A review of technologies for MVDC circuit breakers," in *IECON 2016-42nd Annual Conf. of the IEEE Industrial Electronics Society*. IEEE, 2016, pp. 3799–3805.

[48] F. A. Kharanaq, A. Emadi, and B. Bilgin, "Modeling of conducted emissions for emi analysis of power converters: State-of-the-art review," *IEEE Access*, vol. 8, pp. 189 313–189 325, 2020.

[49] G. R. Papas, N. Titchener, B. M. Yutko, C. Church, and J. L. Tian, "Mechanically-distributed propulsion drivetrain and architecture," Sep. 16 2021, uS Patent App. 17/332,085.

[50] L. Leifsson, A. Ko, W. H. Mason, J. A. Schetz, B. Grossman, and R. Haftka, "Multidisciplinary design optimization of blended-wing-body transport aircraft with distributed propulsion," *Aerospace Science and Technology*, vol. 25, no. 1, pp. 16–28, 2013.

[51] M. A. Gallani, L. C. Góes, and L. A. Nerosky, "Effects of distributed electric propulsion on the performance of a general aviation aircraft," in *2020 AIAA/IEEE Electric Aircraft Technologies Symposium (EATS)*. IEEE, 2020, pp. 1–16.

[52] S. Clarke, M. Redifer, K. Papathakis, A. Samuel, and T. Foster, "X-57 power and command system design," in *2017 IEEE Transportation Electrification Conf. and Expo (ITEC)*. IEEE, 2017, pp. 393–400.

[53] M. J. Armstrong, "Mechanically and electrically distributed propulsion," Jun. 23 2020, uS Patent 10,689,082.

[54] P. Gemin, T. Kupiszewski, A. Radun, Y. Pan, R. Lai, D. Zhang, R. Wang, X. Wu, Y. Jiang, S. Galioto *et al.*, "Architecture, voltage, and components for a turboelectric distributed propulsion electric grid (AVC-TeDP)," *National Aeronautics and Space Administration*, 2015.

[55] B. Łukasik, "Turboelectric distributed propulsion system as a future replacement for turbofan engines," in *Turbo Expo: Power for Land, Sea, and Air*, vol. 50770. American Society of Mechanical Engineers, 2017, p. V001T01A017.

[56] A. O. T. Izaguirre, L. M. G.-C. González, P. Q. Igeño, and P. V. Martínez, "Series-hybridisation, distributed electric propulsion and boundary layer ingestion in long-endurance, small remotely piloted aircraft: Fuel consumption improvements," *Aerospace Science and Technology*, vol. 120, p. 107227, 2022.

[57] H.-J. Steiner, P. C. Vratny, C. Gologan, K. Wieczorek, A. T. Isikveren, and M. Hornung, "Optimum number of engines for transport aircraft employing electrically powered distributed propulsion," *CEAS Aeronautical Journal*, vol. 5, no. 2, pp. 157–170, 2014.

[58] N. K. Borer, M. D. Patterson, J. K. Viken, M. D. Moore, J. Bevirt, A. M. Stoll, and A. R. Gibson, "Design and performance of the NASA SCEPTOR distributed electric propulsion flight demonstrator," in *16th AIAA Aviation Technology, Integration, and Operations Conf.*, 2016, p. 3920.

[59] K. R. Moore and A. Ning, "Distributed electric propulsion effects on existing aircraft through multidisciplinary optimization," in *2018 AIAA/ASCE/AHS/ASC Structures, Structural Dynamics, and Materials Conf.*, 2018, p. 1652.

[60] D. L. Simon, J. W. Connolly, and D. E. Culley, "Control technology needs for electrified aircraft propulsion systems," in *Turbo Expo: Power for Land, Sea, and Air*, vol. 58677. American Society of Mechanical Engineers, 2019, p. V006T05A022.

[61] P. Kou, J. Wang, and D. Liang, "Powered yaw control for distributed electric propulsion aircraft: A model predictive control approach," *IEEE Trans. on Transportation Electrification*, 2021.

[62] E. Nguyen Van, P. Troillard, J. Jézégou, D. Alazard, P. Pastor, and C. Döll, "Reduction of vertical tail using differential thrust: Influence on flight control and certification," *AEGATS'18, Toulouse, France*, pp. 1–8, 2018.

[63] L. Weng, X. Zhang, T. Yao, F. Bu, and H. Li, "A thrust cooperative control strategy of multiple propulsion motors for distributed electric propulsion aircraft," *World Electric Vehicle Journal*, vol. 12, no. 4, p. 199, 2021.

[64] J. S. Gray and J. R. Martins, "Coupled aeropropulsive design optimisation of a boundary-layer ingestion propulsor," *The Aeronautical Journal*, vol. 123, no. 1259, pp. 121–137, 2019.

[65] F. Berg, J. Palmer, P. Miller, and G. Dodds, "HTS system and component targets for a distributed aircraft propulsion system," *IEEE Trans. on Applied Superconductivity*, vol. 27, no. 4, pp. 1–7, 2017.

[66] J. Welstead and J. L. Felder, "Conceptual design of a single-aisle turboelectric commercial transport with fuselage boundary layer ingestion," in *54th AIAA aerospace sciences meeting*, 2016, p. 1027.

[67] J. Welstead, J. Felder, M. Guynn, B. Haller, M. Tong, S. Jones, I. Ordaz, J. Quinlan, and B. Mason, "Overview of the NASA STARC-ABL (rev. B) advanced concept," in *One Boeing NASA Electric Aircraft Workshop*, no. NF1676L-26767, 2017.

[68] S. Farokhi, *Future propulsion systems and energy sources in sustainable aviation*. John Wiley & Sons, 2020.

[69] S. F. Clark, "AERO QTR_03.12, 787 Propulsion System," [Online], 2012, https://www.boeing.com/commercial/aeromagazine/articles/2012_q3/2/ (accessed Aug. 3,2022).

[70] J. L. Felder, "NASA N3-X with turboelectric distributed propulsion," in *Proc. Disruptive Green Propuls. Technol. Conf.*, 2014, pp. 1–18.

[71] K. P. Duffy and R. H. Jansen, "Turboelectric and hybrid electric aircraft drive key performance parameters," in *2018 AIAA/IEEE Electric Aircraft Technologies Symposium (EATS)*. IEEE, 2018, pp. 1–19.

[72] G. Wortmann, "Electric innovative commuter aircraft, D3.1 hybrid-electric propulsion architecture report," Rolls-Royce, Tech. Rep., 2020.

[73] M. D. Moore, "Distributed electric propulsion (DEP) aircraft," *NASA Langley Research Center*, 2012.

[74] A. Seitz, O. Schmitz, A. T. Isikveren, and M. Hornung, *Electrically powered propulsion: comparison and contrast to gas turbines*. Deutsche Gesellschaft für Luft-und Raumfahrt-Lilienthal-Oberth eV, 2012.

[75] M. J. Smith, *Aircraft noise*. Cambridge University Press, 2004, no. 3.

[76] J. Posey, A. Tinetti, and M. Dunn, "The low-noise potential of distributed propulsion on a catamaran aircraft," in *12th AIAA/CEAS Aeroacoustics Conf. (27th AIAA Aeroacoustics Conf.)*, 2006, p. 2622.

[77] A. Synodinos, R. Self, A. Torija Martinez *et al.*, "Noise assessment of aircraft with distributed electric propulsion using a new noise estimation framework," in *24th International Congress on Sound and Vibration, ICSV 2017*. International Institute of Acoustics and Vibration, IIAV, 2017.

[78] A. Manneville, D. Pilczer, and Z. Spakovszky, "Noise reduction assessments and preliminary design implications for a functionally-silent aircraft," in *10th AIAA/CEAS aeroacoustics Conf.*, 2004, p. 2925.

[79] J. Thomas, "Systems analysis of community noise impacts of advanced flight procedures for conventional and hybrid electric aircraft," Ph.D. dissertation, MIT International Center for Air Transportation, 2020.

[80] K. R. Moore and A. Ning, "Takeoff and performance trade-offs of retrofit distributed electric propulsion for urban transport," *Journal of Aircraft*, vol. 56, no. 5, pp. 1880–1892, 2019.

[81] B. L. Litherland, N. K. Borer, and N. S. Zawodny, "X-57 Maxwell high-lift propeller testing and model development," in *AIAA AVIATION 2021 FORUM*, 2021, p. 3193.

[82] T. Pan, "Aerodynamic analysis for hybrid electric distributed propulsion aircraft," Ph.D. dissertation, University of Leeds, 2020.

[83] M. J. Armstrong, M. Blackwelder, A. Bollman, C. Ross, A. Campbell, C. Jones, and P. Norman, "Architecture, voltage and components for a turboelectric distributed propulsion electric grid, final report," 2015.

[84] G. M. Bravo, N. Praliyev, and Á. Veress, "Performance analysis of hybrid electric and distributed propulsion system applied on a light aircraft," *Energy*, vol. 214, p. 118823, 2021.

[85] A. M. Bollman, M. J. Armstrong, C. E. Jones, P. J. Norman, and S. J. Galloway, "Development of voltage standards for turbo-electric distributed propulsion aircraft power systems," in *2015 International Conf. on Electrical Systems for Aircraft, Railway, Ship Propulsion and Road Vehicles (ESARS)*. IEEE, 2015, pp. 1–6.

[86] M. J. Armstrong and C. A. Ross, "Power and protection considerations for TeDP microgrid systems," *Aircraft Engineering and Aerospace Technology: An International Journal*, 2014.

[87] B. T. Schiltgen and J. Freeman, "Aeropropulsive interaction and thermal system integration within the ECO-150: a turboelectric distributed propulsion airliner with conventional electric machines," in *16th AIAA Aviation Technology, Integration, and Operations Conf.*, 2016, p. 4064.

[88] D. C. Loder, A. Bollman, and M. J. Armstrong, "Turbo-electric distributed aircraft propulsion: Microgrid architecture and evaluation for ECO-150," in *2018 IEEE Transportation Electrification Conf. and Expo (ITEC)*. IEEE, 2018, pp. 550–557.

[89] ESAero. https://www.esaero.com/eco-150-project-information. (accessed Aug. 3,2022).

[90] B. T. Schiltgen and J. Freeman, "ECO-150-300 design and performance: a tube-and-wing distributed electric propulsion airliner," in *AIAA Scitech 2019 Forum*, 2019, p. 1808.

[91] B. Schiltgen, A. R. Gibson, M. Green, and J. Freeman, "More electric aircraft: "tube and wing" hybrid electric distributed propulsion with superconducting and conventional electric machines," SAE Technical Paper, Tech. Rep., 2013.

[92] ONERA, "How can we reduce fuel consumption? DRAGON," June 17, 2019, (accessed Aug. 3, 2022). [Online]. Available: https://www.onera.fr/en/news/how-can-we-reduce-fuel-consumption%3F-dragon#:~:text=How%3F,the%20rear%20of%20the%20aircraft.

[93] P. Schmollgruber *et al.*, "Multidisciplinary exploration of DRAGON: an ONERA hybrid electric distributed propulsion concept," in *AIAA Scitech 2019 Forum*, 2019, p. 1585.

[94] P. Schmollgruber, D. Donjat, M. Ridel, I. Cafarelli, O. Atinault, C. François, and B. Paluch, "Multidisciplinary design and performance of the ONERA hybrid electric distributed propulsion concept (DRAGON)," in *AIAA Scitech 2020 Forum*, 2020, p. 0501.

[95] "EcoPulse™, a new approach to distributed propulsion for aircraft," [Online], https://www.airbus.com/en/innovation/zero-emission/electric-flight/ecopulse (accessed Aug. 3,2022).

[96] "The EcoPulse™ hybrid aircraft demonstrator achieves its first key milestone with success," [Online], https://www.safran-group.com/pressroom/ecopulsetm-hybrid-aircraft-demonstrator-achieves-its-first-key-milestone-success-2020-12-10 (accessed Aug. 3,2022).

[97] "Airbus' high-voltage battery technology prepares for EcoPulse flight test and beyond," [Online], https://www.airbus.com/en/newsroom/news/2022-03-airbus-high-voltage-battery-technology-prepares-for-ecopulse-flight-test (accessed Aug. 3,2022).

[98] A. Sgueglia, P. Schmollgruber, N. Bartoli, O. Atinault, E. Benard, and J. Morlier, "Exploration and sizing of a large passenger aircraft with distributed ducted electric fans," in *2018 AIAA Aerospace Sciences Meeting*, 2018, p. 1745.

[99] A. Sgueglia, P. Schmollgruber, N. Bartoli, E. Benard, J. Morlier, J. Jasa, J. R. Martins, J. T. Hwang, and J. S. Gray, "Multidisciplinary design optimization framework with coupled derivative computation for hybrid aircraft," *Journal of Aircraft*, vol. 57, no. 4, pp. 715–729, 2020.

[100] European Union, "Turbo electRic Aircraft Design Environment (TRADE)," [Online], https://cordis.europa.eu/project/id/755458 (accessed Aug. 3, 2022).

[101] G. Valente, S. Sumsurooah, C. I. Hill, M. Rashed, G. Vakil, S. Bozhko, and C. Gerada, "Design methodology and parametric design study of the on-board electrical power system for hybrid electric aircraft propulsion," in *The 10th International Conf. on Power Electronics, Machines and Drives (PEMD 2020)*, vol. 2020, 2020, pp. 448–454.

[102] G. Cinar, D. N. Mavris, M. Emeneth, A. Schneegans, C. Riediger, Y. Fefermann, and A. Isikveren, "Sizing, integration and performance evaluation of hybrid electric propulsion subsystem architectures," in *55th AIAA Aerospace Sciences Meeting*, 2017, p. 1183.

[103] I. Bolvashenkov, J. Kammermann, A. Rubinraut, H.-G. Herzog, and I. Frenkel, "Vehicle electrification: On water, in air and space," 2022.

[104] J. Kammermann, I. Bolvashenkov, K. Tran, H.-G. Herzog, and I. Frenkel, "Feasibility study for a full-electric aircraft considering weight, volume, and reliability requirements," in *2020 International Conf. on Electrotechnical Complexes and Systems*. IEEE, 2020, pp. 1–6.

[105] F. Gaspari, L. Trainelli, A. Rolando, and I. Perkon, "Concept of modular architecture for hybrid electric propulsion of aircraft," *Mahepa, Nov*, 2017.

[106] E. Dillinger, C. Döll, R. Liaboeuf, C. Toussaint, J. Hermetz, C. Verbeke, and M. Ridel, "Handling qualities of ONERA's small business concept plane with distributed electric propulsion," in *31st Congress of the International Council of the Aeronautical Sciences*, 2018.

[107] J. Hermetz, M. Ridel, and C. Doll, "Distributed electric propulsion for small business aircraft a concept-plane for key-technologies investigations." in *ICAS 2016*, 2016.

[108] tecnam, "P2006T twin engine aircraft," https://www.tecnam.com/aircraft/p2006t/ (accessed Aug. 3, 2022).

[109] P. Della Vecchia, D. Malgieri, F. Nicolosi, and A. De Marco, "Numerical analysis of propeller effects on wing aerodynamic: tip mounted and distributed propulsion," *Transportation research procedia*, vol. 29, pp. 106–115, 2018.

[110] NASA, "X-57 Maxwell," (accessed Aug. 3, 2022). [Online]. Available: https://www.nasa.gov/sites/default/files/atoms/files/x-57-litho-print-v4.pdf

[111] M. Sinnett, "787 no-bleed systems: saving fuel and enhancing operational efficiencies," *Aero Quarterly*, vol. 18, pp. 6–11, 2007.

[112] I. Christou, A. Nelms, I. Cotton, and M. Husband, "Choice of optimal voltage for more electric aircraft wiring systems," *IET Electrical Systems in Transportation*, vol. 1, no. 1, pp. 24–30, 2011.

[113] S. Byahut and A. Uranga, "Power distribution and thermal management modeling for electrified aircraft," in *2020 AIAA/IEEE Electric Aircraft Technologies Symposium (EATS)*. IEEE, 2020, pp. 1–15.

[114] E.-S. E. Shin, "Development of high voltage micro-multilayer multifunctional electrical insulation (mmei) system," in *2019 AIAA/IEEE Electric Aircraft Technologies Symposium (EATS)*. IEEE, 2019, pp. 1–14.

[115] *Financial Assistance Funding Opportunity Announcement, Solicitation on Topics Informing New Program Areas, Modification 20-Final, DE-FOA-0001953*, Advanced Research Projects Agency – Energy (ARPA-E) U.S. Department of Energy, Nov. 2021.

[116] I. Cotton, R. Gardner, D. Schweickart, D. Grosean, and C. Severns, "Design considerations for higher electrical power system voltages in aerospace vehicles," in *2016 IEEE International Power Modulator and High Voltage Conf. (IPMHVC)*. IEEE, 2016, pp. 57–61.

[117] K. Ibrahim, S. Sampath, and D. Nalianda, "Optimal voltage and current selection for turboelectric aircraft propulsion networks," *IEEE Trans. on Transportation Electrification*, vol. 6, no. 4, pp. 1625–1637, 2020.

[118] D. Jackson, S. Belakaria, Y. Cao, J. R. Doppa, and X. Lu, "Machine learning enabled design automation and multi-objective optimization for electric transportation power systems," *IEEE Trans. on Transportation Electrification*, vol. 8, no. 1, pp. 1467–1481, 2021.

[119] P. Kshirsagar, J. Ewanchuk, B. van Hassel, R. Taylor, S. Dwari, J. Rheaume, and C. Lents, "Anatomy of a 20 MW electrified aircraft: Metrics and technology drivers," in *2020 AIAA/IEEE Electric Aircraft Technologies Symposium (EATS)*. IEEE, 2020, pp. 1–9.

[120] S. Biser, M. Filipenko, M. Boll, N. Kastner, G. Atanasov, M. Hepperle, D. Keller, D. Vechtel, and M. Noe, "Design space exploration study and optimization of a distributed turbo-electric propulsion system for a regional passenger aircraft," in *2020 AIAA/IEEE Electric Aircraft Technologies Symposium (EATS)*. IEEE, 2020, pp. 1–27.

[121] C. Perullo, A. Alahmad, J. T. Wen, M. D'Arpino, M. Canova, D. N. Mavris, and M. Benzakein, "Sizing and performance analysis of a turbo-hybrid-electric regional jet for the NASA ULI program," in *2019 AIAA/IEEE Electric Aircraft Technologies Symposium (EATS)*. IEEE, 2019, pp. 1–15.

[122] J. Hoelzen, Y. Liu, B. Bensmann, C. Winnefeld, A. Elham, J. Friedrichs, and R. Hanke-Rauschenbach, "Conceptual design of operation strategies for hybrid electric aircraft," *Energies*, vol. 11, no. 1, p. 217, 2018.

[123] Wright, "Technology," https://www.weflywright.com/ (accessed Aug. 3, 2022).

[124] R. Jansen, C. Bowman, and A. Jankovsky, "Sizing power components of an electrically driven tail cone thruster and a range extender," in *16th AIAA Aviation Technology, Integration, and Operations Conf.*, 2016, p. 3766.

[125] G.-D. Nam, H.-J. Sung, S. J. Lee, M. Park *et al.*, "Conceptual design of an aviation propulsion system using hydrogen fuel cell and superconducting motor," *IEEE Trans. on Applied Superconductivity*, vol. 31, no. 5, pp. 1–7, 2021.

[126] M. A. P. Sebastian, T. J. Haugan, and C. J. Kovacs, "Design and scaling laws of a 40-MW-class electric power distribution system for Liquid-$H_2$ fuel-cell propulsion," in *2021 AIAA/IEEE Electric Aircraft Technologies Symposium (EATS)*. IEEE, 2021, pp. 1–12.

[127] Solar IMpulse Fundation, "Propulsion," https://aroundtheworld.solarimpulse.com/adventure (accessed Aug. 3, 2022).

[128] M. T. Fard and J. He, "Comparison of medium-voltage high-frequency power inverters for aircraft propulsion drives," in *2021 IEEE Energy Conversion Congress and Exposition (ECCE)*. IEEE, 2021, pp. 1599–1605.

[129] J. Palmer and E. Shehab, "Modelling of cryogenic cooling system design concepts for superconducting aircraft propulsion," *IET Electrical Systems in Transportation*, vol. 6, no. 3, pp. 170–178, 2016.

[130] J. Xi, X. Pei, J. Sheng, H. Tanaka, Y. Ichiki, M. Zhang, and W. Yuan, "Experimental test and analysis of AC losses in multifilamentary $MgB_2$ wire," *IEEE Trans. on Applied Superconductivity*, vol. 29, no. 5, pp. 1–5, 2019.

[131] T. Yang, F. Gao, S. Bozhko, and P. Wheeler, "Power electronic systems for aircraft," in *Control of Power Electronic Converters and Systems*. Elsevier, 2018, pp. 333–368.

[132] G. V. Brown, J. J. Trudell, L. W. Kohlman, K. P. Duffy, and F. D. Koci, "Status of analysis and manufacturability of superconducting

wires with low AC losses," *NASA-Technical Memorandum*, pp. 1–38, 2020.

[133] J. Kim, K. Kwon, S. Roy, E. Garcia, and D. N. Mavris, "Megawatt-class turboelectric distributed propulsion, power, and thermal systems for aircraft," in *2018 AIAA Aerospace Sciences Meeting*, 2018, p. 2024.

[134] D. Zhang, J. He, D. Pan, M. Schutten, and M. Dame, "High power density medium-voltage megawatt-scale power converter for aviation hybrid-electric propulsion applications," in *2019 IEEE Energy Conversion Congress and Exposition (ECCE)*. IEEE, 2019, pp. 582–588.

[135] J. He, D. Zhang, and D. Pan, "PWM strategy for MW-scale "SiC+Si" ANPC converter in aircraft propulsion applications," *IEEE Trans. on Industry Applications*, vol. 57, no. 3, pp. 3077–3086, 2021.

[136] T. Sakaguchi, M. Aketa, T. Nakamura, M. Nakanishi, and M. Rahimo, "Characterization of 3.3 kV and 6.5 kV SiC MOSFETs," in *PCIM Europe 2017; International Exhibition and Conf. for Power Electronics, Intelligent Motion, Renewable Energy and Energy Management*, 2017, pp. 1–5.

[137] D. Lawhorn, V. Rallabandi, and D. M. Ionel, "Power electronics powertrain architectures for hybrid and solar electric airplanes with distributed propulsion," in *2018 AIAA/IEEE Electric Aircraft Technologies Symposium (EATS)*. IEEE, 2018, pp. 1–6.

[138] L. Zhang, X. Yuan, X. Wu, C. Shi, J. Zhang, and Y. Zhang, "Performance evaluation of high-power SiC MOSFET modules in comparison to Si IGBT modules," *IEEE Trans. on Power Electronics*, vol. 34, no. 2, pp. 1181–1196, 2018.

[139] A. R. Gnadt, R. L. Speth, J. S. Sabnis, and S. R. Barrett, "Technical and environmental assessment of all-electric 180-passenger commercial aircraft," *Progress in Aerospace Sciences*, vol. 105, pp. 1–30, 2019.

[140] A. VanderMeulen and J. Maurin, "Current source inverter vs. voltage source inverter topology," *Technical Data TD02004004E, Eaton*, pp. 1–8, 2010.

[141] B. Sahan, S. V. Araujo, C. Noeding, and P. Zacharias, "Comparative evaluation of three-phase current source inverters for grid interfacing of distributed and renewable energy systems," *IEEE Trans. on Power Electronics*, vol. 26, no. 8, pp. 2304–2318, 2010.

[142] V. Madonna, G. Migliazza, P. Giangrande, E. Lorenzani, G. Buticchi, and M. Galea, "The rebirth of the current source inverter: Advantages for aerospace motor design," *IEEE Industrial Electronics Magazine*, vol. 13, no. 4, pp. 65–76, 2019.

[143] A. D. Anderson, N. J. Renner, Y. Wang, S. Agrawal, S. Sirimanna, D. Lee, A. Banerjee, K. Haran, M. J. Starr, and J. L. Felder, "System weight comparison of electric machine topologies for electric aircraft propulsion," in *2018 AIAA/IEEE Electric Aircraft Technologies Symposium (EATS)*. IEEE, 2018, pp. 1–16.

[144] A. Nawawi, C. F. Tong, S. Yin, A. Sakanova, Y. Liu, Y. Liu, M. Kai, K. Y. See, K.-J. Tseng, R. Simanjorang *et al.*, "Design and demonstration of high power density inverter for aircraft applications," *IEEE Trans. on Industry Applications*, vol. 53, no. 2, pp. 1168–1176, 2016.

[145] R. Chen *et al.*, "A cryogenically-cooled MW inverter for electric aircraft propulsion," in *2020 AIAA/IEEE Electric Aircraft Technologies Symposium (EATS)*. IEEE, 2020, pp. 1–10.

[146] A. Deshpande, Y. Chen, B. Narayanasamy, Z. Yuan, C. Chen, and F. Luo, "Design of a high-efficiency, high specific-power three-level T-type power electronics building block for aircraft electric-propulsion drives," *IEEE Journal of Emerging and Selected Topics in Power Electronics*, vol. 8, no. 1, pp. 407–416, 2019.

[147] *"APPLICATION NOTE 5SYA 2042-09: Failure rates of IGBT modules due to cosmic rays", ABB, 2019. [Online].*

[148] J. A. Swanke, D. Bobba, T. M. Jahns, and B. Sarlioglu, "Design of high-speed permanent magnet machine for aerospace propulsion," in *2019 AIAA/IEEE Electric Aircraft Technologies Symposium (EATS)*. IEEE, 2019, pp. 1–12.

[149] T. M. Jahns and B. Sarlioglu, "The incredible shrinking motor drive: Accelerating the transition to integrated motor drives," *IEEE Power Electronics Magazine*, vol. 7, no. 3, pp. 18–27, 2020.

[150] A. Akturk, J. McGarrity, N. Goldsman, D. J. Lichtenwalner, B. Hull, D. Grider, and R. Wilkins, "The effects of radiation on the terrestrial operation of SiC MOSFETs," in *2018 IEEE International Reliability Physics Symposium (IRPS)*. IEEE, 2018, pp. 2B–1.

[151] A. Akturk, R. Wilkins, J. McGarrity, and B. Gersey, "Single event effects in Si and SiC power mosfets due to terrestrial neutrons," *IEEE Trans. on Nuclear Science*, vol. 64, no. 1, pp. 529–535, 2016.

[152] C. Felgemacher, S. V. Araujo, P. Zacharias, K. Nesemann, and A. Gruber, "Cosmic radiation ruggedness of Si and SiC power semiconductors," in *2016 28th International Symposium on Power Semiconductor Devices and ICs (ISPSD)*. IEEE, 2016, pp. 51–54.

[153] G. Calderon-Lopez, J. Scoltock, Y. Wang, I. Laird, X. Yuan, and A. J. Forsyth, "Power-dense bi-directional DC–DC converters with high-performance inductors," *IEEE Trans. on Vehicular Technology*, vol. 68, no. 12, pp. 11 439–11 448, 2019.

[154] W. Lee, S. Li, D. Han, B. Sarlioglu, T. A. Minav, and M. Pietola, "A review of integrated motor drive and wide-bandgap power electronics for high-performance electro-hydrostatic actuators," *IEEE Trans. on transportation electrification*, vol. 4, no. 3, pp. 684–693, 2018.

[155] T. Chen, *Wide Bandgap Device-Based Power Converter for Integrated Motor Drive System*. The University of Texas at Dallas, 2020.

[156] A. Morya, M. Moosavi, M. C. Gardner, and H. A. Toliyat, "Applications of wide bandgap (WBG) devices in AC electric drives: A technology status review," in *2017 IEEE International Electric Machines and Drives Conf. (IEMDC)*. IEEE, 2017, pp. 1–8.

[157] F. Luo, Z. Yuan, K. Choksi *et al.*, "High-density motor drive development for electric aircraft propulsion: Cryogenic and non-cryo solutions," in *2022 International Power Electronics Conf. (IPEC-Himeji 2022-ECCE Asia)*. IEEE, 2022, pp. 2130–2134.

[158] A. P. Thurlbeck and Y. Cao, "A mission profile-based reliability modeling framework for fault-tolerant electric propulsion," *IEEE Trans. on Industry Applications*, vol. 58, no. 2, pp. 2312–2323, 2022.

[159] C. Hammer, "The reflective wave phenomena, rev.2," [Online] Application note, EATON.

[160] M. Corduan, M. Boll, R. Bause, M. P. Oomen, M. Filipenko, and M. Noe, "Topology comparison of superconducting AC machines for hybrid electric aircraft," *IEEE Trans. on Applied Superconductivity*, vol. 30, no. 2, pp. 1–10, 2020.

[161] S. S. Kalsi, R. A. Badcock, J. G. Storey, K. A. Hamilton, and Z. Jiang, "Motors employing REBCO CORC and $MgB_2$ superconductors for AC stator windings," *IEEE Trans. on Applied Superconductivity*, vol. 31, no. 9, pp. 1–7, 2021.

[162] S. Venuturumilli, F. Berg, L. Prisse, M. Zhang, and W. Yuan, "DC line to line short-circuit fault management in a turbo-electric aircraft propulsion system using superconducting devices," *IEEE Trans. on Applied Superconductivity*, vol. 29, no. 5, pp. 1–6, 2019.

[163] H. Li, B. Xiang, W. Song, Y. Geng, Z. Liu, J. Wang, X. Pei, and Y. Tu, "Effect of arc chute on DC current interruption by liquid nitrogen in HTS electrical system of distributed propulsion aircraft," *IEEE Trans. on Applied Superconductivity*, vol. 31, no. 5, pp. 1–5, 2021.

[164] A. Elwakeel, Z. Feng, N. McNeill, M. Zhang, B. Williams, and W. Yuan, "Study of power devices for use in phase-leg at cryogenic temperature," *IEEE Trans. on Applied Superconductivity*, vol. 31, no. 5, pp. 1–5, 2021.

[165] P. Cheetham, B. Darbha, S. Telikapalli, C. H. Kim, M. Coleman, and S. Pamidi, "Superconducting DC power distribution networks for electric aircraft," in *2020 AIAA/IEEE Electric Aircraft Technologies Symposium (EATS)*. IEEE, 2020, pp. 1–7.

[166] I. Barnola, D. Freeman, P. Cheetham, S. Yang, C. H. Kim, and S. Pamidi, "Exploring options for integrated cryogenic circulation loop of superconducting power devices on electric aircraft," in *2019 AIAA/IEEE Electric Aircraft Technologies Symposium (EATS)*. IEEE, 2019, pp. 1–8.

[167] Z. Zhang *et al.*, "Characterization of wide bandgap semiconductor devices for cryogenically-cooled power electronics in aircraft applications," in *2018 AIAA/IEEE Electric Aircraft Technologies Symposium (EATS)*. IEEE, 2018, pp. 1–8.

[168] R. Chen and F. F. Wang, "SiC and GaN devices with cryogenic cooling," *IEEE Open Journal of Power Electronics*, vol. 2, pp. 315–326, 2021.

[169] X. Chen, S. Jiang, Y. Chen, H. Gou, Q. Xie, and B. Shen, "Transient modeling and loss analysis of SiC MOSFETs at cryogenic and room temperatures," *IEEE Trans. on Applied Superconductivity*, vol. 31, no. 8, pp. 1–4, 2021.

[170] K. Tian *et al.*, "Comprehensive characterization of the 4H-SiC planar and trench gate mosfets from cryogenic to high temperature," *IEEE Trans. on Electron Devices*, vol. 66, no. 10, pp. 4279–4286, 2019.

[171] H. Y. Gou, Y. Chen, M. G. Tang, R. B. Zhao, X. S. Tan, and L. Yang, "Dynamic-switching energy dissipation behaviors of cryogenic power mosfet at 77 K," *IEEE Trans. on Applied Superconductivity*, vol. 31, no. 8, pp. 1–2, 2021.

[172] J. Qi, X. Yang, X. Li, K. Tian, Z. Mao, S. Yang, and W. Song, "Temperature dependence of dynamic performance characterization of 1.2-kV SiC power MOSFETs compared with Si IGBTs for wide temperature applications," *IEEE Trans. on Power Electronics*, vol. 34, no. 9, pp. 9105–9117, 2018.

[173] K. Hong *et al.*, "Experimental investigations into temperature and current dependent on-state resistance behaviors of 1.2 kV SiC MOSFETs,"

*IEEE Journal of the Electron Devices Society*, vol. 7, pp. 925–930, 2019.

[174] J. Qi, X. Yang, X. Li, W. Chen, T. Long, K. Tian, X. Hou, and X. Wang, "Comprehensive assessment of avalanche operating boundary of SiC planar/trench MOSFET in cryogenic applications," *IEEE Trans. on Power Electronics*, vol. 36, no. 6, pp. 6954–6966, 2020.

[175] R. Ren *et al.*, "Characterization and failure analysis of 650-V enhancement-mode GaN HEMT for cryogenically cooled power electronics," *IEEE Journal of Emerging and Selected Topics in Power Electronics*, vol. 8, no. 1, pp. 66–76, 2019.

[176] K. K. Leong, "Utilising power devices below 100 K to achieve ultra-low power losses," *Ph. D. Thesis*, 2011.

[177] L. Graber *et al.*, "Cryogenic power electronics at megawatt-scale using a new type of press-pack IGBT," in *IOP Conf. Series: Materials Science and Engineering*, vol. 279, no. 1, 2017, p. 012011.

[178] H. Gui *et al.*, "Development of high-power high switching frequency cryogenically cooled inverter for aircraft applications," *IEEE Trans. on Power Electronics*, vol. 35, no. 6, pp. 5670–5682, 2019.

[179] S. Yin *et al.*, "Characterization of inductor magnetic cores for cryogenic applications," in *2021 IEEE Energy Conversion Congress and Exposition (ECCE)*, 2021, pp. 5327–5333.

[180] C. Park, J. Wei, S. Singh, S. Narra, L. Graber, and M. Imperatore, "The characteristics of film capacitors at room temperature and in liquid Nitrogen," in *2018 AIAA/IEEE Electric Aircraft Technologies Symposium (EATS)*. IEEE, 2018, pp. 1–7.

[181] H. Gui *et al.*, "Review of power electronics components at cryogenic temperatures," *IEEE Trans. on power electronics*, vol. 35, no. 5, pp. 5144–5156, 2019.

[182] M. Hoogreef, R. Vos, R. de Vries, and L. L. Veldhuis, "Conceptual assessment of hybrid electric aircraft with distributed propulsion and boosted turbofans," in *AIAA Scitech 2019 Forum*, 2019, p. 1807.

[183] "High energy density lithium-ion cells with silicon nanowire anode technology," [Online], https://www1.grc.nasa.gov/wp-content/uploads/5.-Amprius.pdf (accessed Aug. 3,2022).

[184] G. Soloveichik, "Electrified future of aviation: Batteries or fuel cells," *The Advanced Research Projects Agency–Energy (ARPA-E): Washington, DC, USA*, 2019.

[185] M. Alkali, M. Y. Edries, A. R. Khan, H. Masui, and M. Cho, "Design considerations and ground testing of electric double-layer capacitors as energy storage components for nanosatellites," *Journal of small satellites*, vol. 4, no. 2, pp. 387–405, 2015.

[186] G. Bossi, A. Damiano, N. Campagna, V. Castiglia, R. Miceli, and A. Di Tommaso, "A hybrid storage systems for all electric aircraft," in *2021 IEEE 15th International Conf. on Compatibility, Power Electronics and Power Engineering*, 2021, pp. 1–6.

[187] J. M. Collins and D. McLarty, "All-electric commercial aviation with solid oxide fuel cell-gas turbine-battery hybrids," *Applied Energy*, vol. 265, p. 114787, 2020.

[188] P. J. Ansell and K. S. Haran, "Electrified airplanes: A path to zero-emission air travel," *IEEE Electrification Magazine*, vol. 8, no. 2, pp. 18–26, 2020.

[189] H. Li, T. Yao, X. Zhang, F. Bu, and L. Weng, "Hybrid energy storage management strategy for electric propulsion aircraft based on three-step power distribution," *World Electric Vehicle Journal*, vol. 12, no. 4, p. 209, 2021.

[190] B. Guddanti, J. Choi, M. Illindala, and R. Roychowdhury, "Effect of endogenous failure events on the survivability of turboelectric distributed propulsion system," *IEEE Trans. on Industry Applications*, 2021.

**Majid T. Fard** (S'19) received the B.Sc. and M.Sc. degrees (both with Hons) in electrical engineering with an emphasis on power energy conversion and renewable energies from the University of Tabriz, Iran in 2013 and 2016, respectively. He is currently working toward the Ph.D. degree in electrical engineering at the University of Kentucky, KY, USA. He previously worked in the industry, as an R&D Engineer and Project Manager at the IKCO automotive company in Iran. His research interests include high efficiency and high power-density propulsion drives for more-electric aircraft systems, fault-tolerant electric power converters for safety-critical applications, and transportation electrification.

**JiangBiao He** (S'08, M'15, SM'16) is with the Department of Electrical and Computer Engineering, University of Kentucky, USA. He previously worked in industry, most recently as a Lead Engineer at GE Global Research, Niskayuna, New York. He also worked at Eaton Corporation and Rockwell Automation before he joined GE in 2015. He received the Ph.D. degree in electrical engineering from Marquette University, Wisconsin, USA. His research interests include transportation electrifications particularly on electric aircraft propulsion, renewable energies, and fault-tolerant electric power apparatuses for safety-critical applications. He has authored and co-authored over 120 technical papers and 10 U.S. patents. He is an IEEE Senior Member, and has served as an Editor or Associate Editor for several prestigious IEEE journals in the electric power area. He also served in various roles in the organizing committees for numerous IEEE conferences, and has been an active member of multiple IEEE standards working groups. He is the recipient of the 2019 AWS Outstanding Young Member Achievement Award recognized by the IEEE Industry Applications Society.

**Hao Huang** (F'14) is the Retired Technology Chief of GE Aviation—Electrical Power since May of 2020. He was responsible for generating the technical directions, innovation strategies, and multi-generation product roadmaps for the GE aircraft electrical power division. He was constantly leading and contributing innovations and inventions of aircraft electrical power technologies. Currently, he is a distinguished adjunct professor in the University of Houston, and an adjunct professor in WEMPEC of the University of Wisconsin – Madison. Dr. Huang is a NAE Member, IEEE fellow, and SAE fellow. He received his Ph.D. Degree in Electrical Engineering from the University of Colorado at Boulder, Boulder, Colorado, USA in 1987. He has 35 years of experience in Aircraft Electrical Power Systems, Power Generations, Engine Starting, Power Electronics and Controls, and Electric Vehicle Drives. He has had 80 US patents including pending and multiple technical publications in the above-mentioned areas. Dr. Hao Huang is the winner of 2019 IEEE Transportation Technologies Award.

**Yue Cao** (Member, IEEE) received the B.S. degree (Hons.) in electrical engineering with a second major in mathematics from the University of Tennessee, Knoxville, TN, USA, in 2011, and the M.S. and Ph.D. degrees in electrical engineering from the University of Illinois at Urbana–Champaign (UIUC), Champaign, IL, USA, in 2013 and 2017, respectively. Dr. Cao is currently an Assistant Professor with the Energy Systems Group at Oregon State University (OSU), Corvallis, OR, USA. Before joining OSU, he was a Research Scientist with the Propulsions Team at Amazon Prime Air in Seattle, WA, USA. He was a Power Electronics Engineer Intern with Special Projects Group at Apple Inc., Cupertino, CA, USA; Halliburton Company, Houston, TX, USA; and Oak Ridge National Laboratory, TN, USA. He was a Sundaram Seshu Fellow in 2016 at UIUC, where he was a James M. Henderson Fellow in 2012. His research interests include power electronics, motor drives, and energy storage with applications in renewable energy integration and transportation electrification. Dr. Cao was a national finalist of the USA Mathematical Olympiad (USAMO) in 2006 and 2007. He received the Myron Zucker Student Award from the IEEE Industry Applications Society (IAS) in 2010. He won the Oregon State Learning Innovation Award for transformative education in 2020. He is a recipient of the 2022 NSF CAREER award. He is selected into National Academy of Engineering (NAE) Frontier of Engineering (FOE) class of 2022. Dr. Cao is currently the Special Sessions Chair of the 2022 IEEE Energy Conversion Congress Expo (ECCE) and was the Tutorials Chair of 2021 ECCE. He is a board member and Award Chair of IEEE Power Electronics Society (PELS) TC11 – Aerospace Power. In 2020, he helped establish an IEEE PELS Chapter at OSU. He is currently an Associate Editor for IEEE Transactions on Transportation Electrification and an Associate Editor for IEEE Transactions on Industry Applications.